



**NAYAN NAGESH NAYAK**

Graduated in Biochemical Engineering

**DEVELOPMENT OF MIXED MATRIX  
MEMBRANES WITH METAL-ORGANIC  
FRAMEWORKS AND IONIC LIQUIDS  
FOR BIOGAS UPGRADING**

Dissertation for obtaining the Erasmus Mundus Master degree  
in Membrane Engineering

Advisor: Luísa Neves, Post - Doc Researcher, FCT-UNL  
Co-advisor(s): Isabel Coelho, Professor, FCT-UNL  
João G. Crespo, Professor, FCT-UNL

Jury:

President: Prof. Isabel Coelho, Assistant Professor, FCT, UNL, Lisboa, Portugal  
Examiner(s): Dr. Vitor Alves, Assistant Researcher, ISA, UTL, Portugal  
Prof. André Ayrál, Professor, UM2, Montpellier, France  
Prof. Karel Bouzek, Professor, VŠCHT, Prague, Czech Republic  
Prof. Patrice Bacchin, Professor, UPS, Toulouse, France  
Member(s): Dr. Luísa Neves, Post-Doc Researcher, FCT, UNL, Lisboa, Portugal

**NAYAN NAGESH NAYAK**

Graduated in Biochemical Engineering

**DEVELOPMENT OF MIXED  
MATRIX MEMBRANES WITH  
METAL - ORGANIC  
FRAMEWORKS AND IONIC  
LIQUIDS FOR BIOGAS  
UPGRADING**

Dissertation presented to Faculdade de  
Ciências e Tecnologia, Universidade Nova  
de Lisboa for obtaining the master degree in  
Membrane Engineering

**July 2013**

Development of Mixed Matrix Membranes with Metal – Organic Frameworks and Ionic Liquids for Biogas Upgrading



The EM3E Master is an Education Programme supported by the European Commission, the European Membrane Society (EMS), the European Membrane House (EMH), and a large international network of industrial companies, research centers and universities (<http://www.em3e.eu>).

Copyright @ Nayan Nagesh Nayak, FCT/UNL

A Faculdade de Ciências e Tecnologia e a Universidade Nova de Lisboa têm o direito, perpétuo e sem limites geográficos, de arquivar e publicar esta dissertação através de exemplares impressos reproduzidos em papel ou de forma digital, ou por qualquer outro meio conhecido ou que venha a ser inventado, e de a divulgar através de repositórios científicos e de admitir a sua cópia e distribuição com objectivos educacionais ou de investigação, não comerciais, desde que seja dado crédito ao autor e editor.

Projecto financiado com o apoio da Comissão Europeia. A informação contida nesta publicação vincula exclusivamente o autor, não sendo a Comissão responsável pela utilização que dela possa ser feita.

## **Acknowledgements**

*“If I have seen further than others, it is because I am standing on the shoulders of giants”*

*- Sir Isaac Newton*

And they certainly were giants who let me climb their shoulders and stand there long enough to see a little further than what I had seen before. I pay a humble tribute by dedicating this work to them.

I express my heartfelt gratitude to my supervisor, Dr. Luísa Neves, Research Associate, Chemical and Biochemical Engineering Department at Faculdade de Ciências e Tecnologia, Universidade Nova de Lisboa, for her vision, motivation, encouragement, and moral support throughout this project.

I express my sincere thanks to my co - supervisors Prof. Isabel Coelho and Prof. João G. Crespo, Professors at Chemical and Biochemical Engineering Department at Faculdade de Ciências e Tecnologia, Universidade Nova de Lisboa, for their keen observations, critical judgement and invaluable advice at the right moment which helped me complete this project.

I also thank Hugo Andrade, Rita Ferreira, Ana Rute Ferreira, Carla Martins and Inês Meireles, for helping me with the experiments and giving me useful practical advice and on the whole making my work at DQ, FCT-UNL highly enjoyable. I am thankful to Prof. Vitor Alves, Professor, Instituto Superior de Agronomia, Lisbon, for his help with experiments regarding the mechanical properties.

I would like to sincerely thank Dr. Elena Vallejo, Chargée de Projets, UM2, France for bearing with us, being so kind and listening to all our problems for the last two years and helping us above and beyond her capacity on many occasions

I am also very grateful to all the professors and especially to the coordinator of the EM3E program Prof. André Ayrál for his support and guidance throughout the entire master course.

I also thank all the faculty, research and administrative staff of UM2 - France, ICT – Prague and FCT-UNL- Portugal for providing the necessary support either directly or indirectly.

I would like to thank the European Union and the European Commission for organizing the Erasmus Mundus scholarship program without which I couldn't have been able to do this course.

Lastly, I would like to thank my wife, Divya and my parents for their patience and everlasting support throughout the duration of this course. It would not have been possible without their love, consideration and understanding.



## ***Abstract***

Biogas is produced as a result of anaerobic degradation of organic matter and consists of approximately 60% methane and 40% CO<sub>2</sub> and other impurities. Pure methane is a high calorific fuel with great commercial value. The presence of impurities reduces its combustion efficiency. Also in order to be transportable methane needs to be compressed which is not possible if CO<sub>2</sub> is present. Thus it makes sense to upgrade biogas in order to enhance its commercial value. Biogas upgrading by membrane based gas separation processes offer a number of benefits over other gas separation technologies namely, low energy expense, small footprint and lack of mechanical complexity. Presently several membrane based processes are being applied for this purpose but have still not reached the commercial popularity of existing processes like Pressure swing adsorption or Water scrubbing. This is mainly because of lower permeability and selectivity of affordable membranes and hence lower throughput and productivity.

Currently several research efforts are being made to develop better membranes – one such type are mixed matrix membranes. Several additives/fillers could be added or dispersed in the matrix to make mixed matrix membranes, the most popular being inorganic molecules like zeolites and more recently, metal organic frameworks (MOFs). In parallel, several research efforts are focused on developing supported ionic liquid membranes (SILMs) - membranes impregnated with ionic liquid in pores which have shown promise for separation of both CO<sub>2</sub>/N<sub>2</sub> and CO<sub>2</sub>/CH<sub>4</sub> gas pairs. However, as the ionic liquid is retained in the porous support merely by capillary forces, these membranes are not stable for high pressure applications (e.g., separation of CO<sub>2</sub>/CH<sub>4</sub>).

In the present work attempts have been made to solve this problem by synthesizing ionic liquid incorporated dense Matrimid membranes. In such membranes the ionic liquid is impregnated inside a dense membrane by a physico-chemical interaction like cross-linking achieved by careful selection of polymerization environment i.e., the solvent and physical conditions. These membranes showed better hydrophilicity than neat Matrimid but lower puncture resistance. On incorporation of increasing levels of ionic liquid in the membrane (80% wt/wt of Matrimid) the CO<sub>2</sub> permeability increased upto 36 barrer, which is better than that of neat Matrimid but not beyond the referenced Robeson upper bound cited in the literature. However the CO<sub>2</sub>/CH<sub>4</sub> selectivity decreased to 7.5.

To further improve the selectivity, efforts have been made to develop ionic liquid incorporated mixed matrix membrane with dispersed MOFs. Three different MOFs – MIL 101, MOF-5 and Cu<sub>3</sub>(BTC)<sub>2</sub>, which were reported in literature to have high CO<sub>2</sub>/CH<sub>4</sub> separation capacity were used at a loading of

20%. It was found that the selectivity further reduced (MIL 101- 3, MOF 5 – 5 and  $\text{Cu}_3(\text{BTC})_2 - 0.29$ ) but in case of  $\text{Cu}_3(\text{BTC})_2$  based membrane the  $\text{CO}_2$  permeability increased to 240 barrer and  $\text{CH}_4$  permeability increased to 843 barrer. From these results it can be said that further studies with different MOF loadings and task specific ionic liquids could lead to discovery of better membrane for high performance  $\text{CO}_2/\text{CH}_4$  separation for biogas upgrading.

**Keywords:** Biogas upgrading, mixed matrix membrane, Matrimid, ionic liquids, metal organic frameworks, biomethane.

# ***Table of Contents***

## ***Contents***

Acknowledgements .....	i
Abstract .....	ii
List of figures .....	vi
List of tables .....	vii
Abbreviations .....	viii
1. Introduction .....	1
1.1. Motivation .....	1
1.2. Goal and objectives .....	2
2. Literature Review .....	3
2.1. Biogas .....	3
2.2. Biogas Upgrading – Conventional methods .....	4
2.3. Membrane based biogas upgrading .....	5
2.4. Economics of biogas upgrading .....	14
3. Materials and Methods .....	17
3.1. Membrane preparation.....	17
3.2. Contact Angle.....	18
3.3. Scanning Electron Microscopy (SEM).....	19
3.4. Mechanical Properties .....	19
3.4.1. Puncture test .....	19
3.5. Gas Permeability .....	20

4. Results and Discussions .....	22
4.1. Membrane Preparation .....	22
4.2. Surface Properties.....	22
4.2.1. Contact Angle.....	22
4.3. Scanning Electron Microscopy (SEM).....	24
4.4. Mechanical Properties .....	30
4.4.1. Puncture test .....	30
4.5. Gas Permeability .....	32
5. Conclusions and Future Perspectives .....	36
6. References .....	38
7. Appendix .....	I
7.1. Appendix I: Estimation of $\beta$ .....	I
7.2. Appendix II: Gas Permeation Estimation and Pressure profiles .....	II
7.3. Appendix III: Puncture test – Stress vs Strain curves.....	III

## List of Figures

Figure No.	Figure title	Page
Figure 2.1	Biogas Lifecycle	4
Figure 2.2	Biogas upgrading systems in Europe (a) number; (b) overall capacity	6
Figure 2.3	Structure of Matrimid <sup>®</sup> 5218	9
Figure 2.4	Chemical structure of (a) [emim][Tf <sub>2</sub> N] and (b) [bmim][Tf <sub>2</sub> N]	10
Figure 2.5	Structural representation of (a) MOF 5 (b) Cu <sub>3</sub> (BTC) <sub>2</sub> and (c) MIL 101	12
Figure 3.1	Scheme of method of membrane preparation	17
Figure 3.2	Schematic of a sessile drop, contact angle and the three interfacial tensions are shown	18
Figure 3.3	Puncture Test Scheme	20
Figure 3.4	Gas permeation setup; V1, V4 are inlet valves; V2, V3 are exhaust valves; P11, P12 are the pressure transducers. The whole setup is placed in a thermostatic water bath	21
Figure 4.1	Contact angle for membranes with different IL contents	23
Figure 4.2	Scanning Electron Microscopy images of the Matrimid membranes with different IL %	27
Figure 4.3	SEM images of the Matrimid membranes with 50% IL and 20% MOFs - Cu <sub>3</sub> (BTC) <sub>2</sub> , MIL101 and MOF-5 with Secondary electron emission (SE) and Back-scattered electron emission mode (BSE)	29
Figure 4.5.1	CO <sub>2</sub> / CH <sub>4</sub> Permeability with increasing Ionic liquid content	33
Figure 4.5.2	Complete Robeson plot for CO <sub>2</sub> /CH <sub>4</sub> with results from the current work	34
Figure 7.1	Feed and Permeate Pressure Profiles in the permeation cell	I
Figure 7.2	Graphical representation of Eq 3.5.1 where the slope gives the value of $\beta$	I
Figure 7.3	Feed and Permeate pressure profile for CO <sub>2</sub> with Matrimid membrane	II
Figure 7.4	CO <sub>2</sub> permeance in Matrimid membrane	II
Figure 7.5	Stress Vs. Strain Curve for Matrimid membrane	III
Figure 7.6	Stress Vs. Strain Curve for Matrimid +25% IL membrane	IV
Figure 7.7	Stress Vs. Strain Curve for Matrimid 80% IL membrane	IV
Figure 7.9	Stress Vs. Strain Curve for Matrimid + 50% IL + 20% Cu <sub>3</sub> (BTC) <sub>2</sub>	V

## *List of Tables*

<b>Table No.</b>	<b>Table title</b>	<b>Page</b>
Table 2.1	Composition of Biogas	3
Table 2.2	Details about some popular MOFs which are being researched worldwide.	13
Table 2.3	Biogas upgrading plants operating equipment from the manufacturers	15
Table 2.4	Comparison of demands for the most common technologies at large and small scale	15
Table 3.1	Example of the quantities of components added to make the membranes	18
Table 4.4.1	Puncture test stress - strain data with membrane thickness for varied IL loading	30
Table 4.4.2	Puncture test stress - strain data with membrane thickness for membranes with MOFs and IL	31
Table 4.5.1	Membrane Permeation data	32

## List of Abbreviations

$\alpha_{CO_2/CH_4}$	Membrane Selectivity of CO <sub>2</sub> over CH <sub>4</sub>
$[B(CN)_4]$	Tetracyanoborate
$[BF_4]$	Tetrafluoroborate
<i>bmim</i>	1-Butyl-3-methylimidazolium
<i>CA</i>	Cellulose Acetate
<i>CH<sub>4</sub></i>	Methane
<i>CO<sub>2</sub></i>	Carbon dioxide
$Cu_3(BTC)_2$	Copper benzene-1,3,5-tricarboxylate
<i>DTDA-DAPI</i>	poly(3,3',4,4' benzophenone tetracarboxylic - dianhydride diaminophenylindane)
<i>emim</i>	1-ethyl-3-methylimidazolium
<i>EU</i>	European Union
<i>6FDA</i>	2,2'-Bis (3,4-Dicarboxyphenyl) Hexafluoropropane Dianhydride
<i>FTIR</i>	Fourier Transform InfraRed Spectroscopy
<i>GPU</i>	Gas Permeation Unit
<i>H<sub>2</sub></i>	Hydrogen
<i>H<sub>2</sub>O</i>	Water
<i>H<sub>2</sub>S</i>	Hydrogen Sulfide
<i>IL</i>	Ionic Liquid
<i>MIL</i>	Chromium terephthalate
<i>MMM</i>	Mixed Matrix Membrane
<i>MOF</i>	Metal Organic Framework
<i>N<sub>2</sub></i>	Nitrogen
$P_{CH_4}$	Permeability of methane
$P_{CO_2}$	Permeability of carbon dioxide
<i>PDMS</i>	Polydimethylsiloxane
<i>PI</i>	Polyimide
$[PF_6]$	hexafluorophosphate
<i>PSA</i>	Pressure Swing Absorption
<i>PVA</i>	Polyvinylacetate
<i>RTIL</i>	Room Temperature Ionic Liquid
<i>SILM</i>	Supported Ionic Liquid Membrane
$[Tf_2N]$	bis(trifluoromethylsulfonyl)imide
$T_g$	Glass transition temperature
<i>vbim</i>	1-vinyl-3-butylimidazolium
<i>ZIF</i>	Zeolitic Imidazolate Framework
<i>THF</i>	Tetrahydrofuran
<i>SEM</i>	Scanning Electron Microscopy
<i>% wt.</i>	Weight percentage

---

# 1. INTRODUCTION

---



## **1.1. Motivation**

Methane and hydrogen are two gases with great potential and both can be renewably produced by biological systems. These gases are produced as an offshoot of waste degradation. However, they are produced as part of a mixture and need to be cleaned or stripped. Biogas, for example, produced as a result of anaerobic degradation of organic matter consists of approximately 60% methane and 40% CO<sub>2</sub> and other impurities [1]. Pure methane is a high calorific fuel with great commercial value. The presence of impurities reduces its combustion efficiency. Also in order to be transportable methane needs to be compressed which is not possible if CO<sub>2</sub> is present. Thus it makes sense to upgrade biogas in order to enhance its commercial value.

In order to upgrade biogas, membrane based gas separation processes offer a number of benefits over other gas separation technologies namely, low energy expense, small footprint and lack of mechanical complexity. The first CO<sub>2</sub> separation membrane introduced in an industrial process was the anisotropic cellulose acetate membrane developed by Grace Membrane Systems in the late 1970s [2]. A high-performance gas separation material requires both high permeability and high selectivity; however, it is hard to achieve both at the same time. Dense polyimide membranes are well known for their high CO<sub>2</sub> selectivity. Matrimid is a commercially available polyimide material which is popular because of its ease of polymerization and economical pricing. It is also inherently, moderately selective and permeable to CO<sub>2</sub> [3]. This aspect of Matrimid can be improved upon by creating a hybrid or mixed matrix membrane with gas or molecule selective particles dispersed in the polymer. Several efforts have been made on this front by dispersing gas selective zeolites and metal organic frameworks (MOFs) in Matrimid to improve its performance [4, 5].

In the past two decades, ionic liquids (ILs) have become a research focus due to their unique combination of properties such as negligible vapour pressure, tuneable solvation properties and high ionic conductivities. More recently, ILs have been explored as new CO<sub>2</sub> separation media, largely due to their highly preferential solubility for CO<sub>2</sub> over other gases such as N<sub>2</sub> and CH<sub>4</sub> [6, 7]. Previous studies using SILMs (Supported Ionic liquid membranes – membranes impregnated with ionic liquid in pores) showed promise for separation of both CO<sub>2</sub>/N<sub>2</sub> and CO<sub>2</sub>/CH<sub>4</sub> gas pairs [8, 9, 10]. However, as the ionic liquid is retained in the porous support merely by capillary forces, these membranes are not stable for high pressure applications (e.g., separation of CO<sub>2</sub>/CH<sub>4</sub>).

In the present study, a simple approach to solve the above mentioned problems has been attempted by preparing ionic liquid incorporated dense matrimid membranes. In such membranes the ionic liquid is impregnated inside a dense membrane by a physico - chemical interaction like cross-linking achieved by careful selection of polymerization environment i.e., the solvent and physical conditions [11]. In most cases such membranes exhibit properties which are midway between SILMs

and dense gas separation membranes. They also show improved mechanical and thermal properties in comparison to the former. Furthering these concepts, efforts have also been made to develop ionic liquid incorporated mixed matrix membrane with dispersed metal organic frameworks (MOFs) particles with the potential objective of using it for high performance biogas upgrading.

## **1.2. Goal and objectives**

The primary goal of this work is to synthesize a mixed matrix membrane containing an ionic liquid and MOF particles which can be used for separation of carbon dioxide from biogas to obtain a stream of pure bio-methane.

In order to achieve this goal the tasks were divided into the following objectives:

- Standardization of polymerization conditions for chosen polymer i.e., Matrimid;
- Screening of suitable Ionic liquids and MOFs based on data available in literature;
- Synthesis of mixed matrix membranes with different ionic liquid loading;
- Selection of appropriate Ionic liquid loading based on permeation properties;
- Synthesis and analysis of mixed matrix membrane containing ionic liquid and MOFs.

---

## 2. LITERATURE REVIEW

---

## 2.1. Biogas

Biogas production is a process which uses anaerobic conditions together with microorganisms and organic substrates in order to produce a mixture of gases; mainly carbon dioxide and bi-methane. Organic substrates that can be used as a feedstock are energy crops, manures, industrial wastes, sewage sludge, and the organic fraction of municipal solid wastes. Biogas is produced naturally via many processes such as rice paddies, marshes and ruminants. Biogas can also be produced in engineered systems such as; anaerobic digestion, sewage plants and landfills. Table 2.1 shows the composition of the raw biogas.

**Table 2. 1. Composition of Biogas [1]**

<b>Gas</b>	<b>Percentage</b>
<b>Methane</b>	50-75
<b>Carbon dioxide</b>	25-45
<b>Water vapour</b>	1-2
<b>Carbon monoxide</b>	0-0.3
<b>Nitrogen</b>	1-5
<b>Hydrogen</b>	0-3
<b>Hydrogen sulphide</b>	0.1-0.5
<b>Oxygen</b>	Trace

The production of biogas is economically and environmentally beneficial as it involves the conversion of biomass into methane and carbon dioxide. It is beneficial to remove methane and carbon dioxide as they are both considered greenhouse gases which have a negative impact on the environment. The produced biogas can be used for heat and/or power generation, vehicle fuel and for national grid injection when upgraded. Figure 2.1 shows a general overview of Biogas lifecycle.

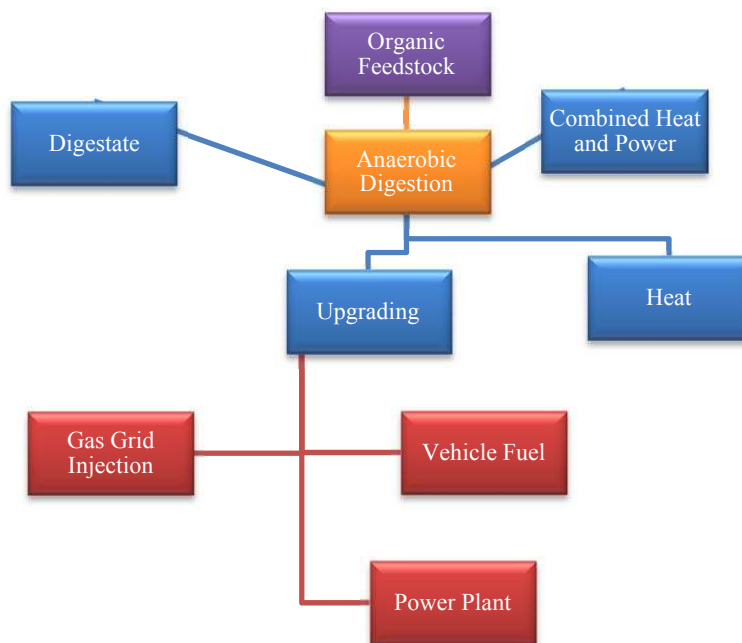


Figure 2. 1. Biogas Lifecycle [1]

There is an increasing demand for upgraded biogas, fuelled by an ever growing concern for the environment, climate change and air qualities especially in the urban environment. The European Union is predicted to be responsible for 21 % of the greenhouse gas emissions globally [12, 13].

Bio-methane production can be used to provide fuel and heat source to promote regional development, as it is more eco-friendly than the extraction of fossil fuels. An important consideration for implementing the use of bio-methane production is that the feedstock is available all year around [14]. Raw biogas can be combusted in a boiler though it does have a lower calorific value. However, it is necessary to reduce CO<sub>2</sub> levels below 2 vol% from biogas because it has no heating value and it causes corrosion in process equipment when in the presence of water (formation of carbonic acid). Upgraded biogas, on the other hand, can be used as a vehicle fuel, material for the chemical industry, reactor fuel for the heat and electricity generating industry or for injection to the national gas supply grid. Though upgraded biogas can be used in many ways, raw biogas use is still the most common option and the most economically viable [15].

## 2.2. Biogas Upgrading – Conventional methods

Upgrading essentially involves reduction of CO<sub>2</sub> levels to the range of 2 – 5 % (by volume) in stock biogas. There are several standardized and popular methods to do this on the European market. The water scrubber and pressure swing adsorption being the most common currently, since both methods are more technically matured [16]. Cleaning and upgrading technologies that are selected for plants are dependent upon several factors, one of them being the gas quality required [16].

Water scrubbing is used to separate both CO<sub>2</sub> and H<sub>2</sub>S from biogas owing to their higher solubility in water than H<sub>2</sub> and CH<sub>4</sub>. Generally, the biogas and water jet are fed to a packed column (typically, high surface area plastic media) in countercurrent mode. The water cannot be recycled [15]. Polyethylene glycol absorption is similar to the water scrubbing process, but with the water replaced by a better suited solvent (e.g. The Lurgi Purisol process and UOP Selexol process).

PSA (Pressure swing adsorption) is a technology where gases are separated under pressure which is dependent on their ability to penetrate the material and remove the unwanted contaminant(s). PSA technology is very flexible and can absorb a broad range of contaminants in gases or liquids [15]. Zeolites (highly porous) are the most common commercial adsorbent which acts as molecular sieves [14]. The absorbed gases are then desorbed from the zeolites by decreasing the pressure, allowing regeneration [14], hence the name, Pressure swing adsorption. Other popular adsorbents are activated carbon, carbon molecular sieves etc. that are suitable to separate a number of different gaseous compounds from biogas.

Cryogenic separation is based on fractional distillation. The raw biogas is compressed in multiple stages with intercooling which allow the gas to be further compressed each time. The compressed gas is dried to avoid freezing in the following cooling process. The gas is cooled to approximately -55 °C by heat exchangers. The pressure is then altered and the temperature is decreased to -110 °C. The gas phase, which consists of more than 97% methane, is heated before it leaves the plant [17, 15]. CO<sub>2</sub> is separated by condensation either by lowering the temperature or increasing the pressure.

Membrane separation processes for CO<sub>2</sub> removal generally provide several advantages over the above-mentioned conventional separation techniques including low capital cost, high energy efficiency, ease of processing, simple process equipment, and relative ease to operate and control. Polymeric membranes, such as UOP Separex cellulose acetate (CA) membranes, have already proven to operate successfully for natural gas upgrading [4].

### ***2.3. Membrane based biogas upgrading***

Gas separation membrane systems have been widely recommended due to their simplicity, modular nature, and attractive economics compared to more traditional separation technologies such as pressure swing adsorption (PSA) and cryogenic distillation. The concept of membrane separation is based on the principle that only selected components of a mixture of fluids are able to pass through a barrier (i.e. membrane). The separation of a vapor/gas(es) mixture is driven by the chemical potential (or pressure) difference of the components across the membrane. When a stream of vapor/gas mixture is fed to the upstream side of the membrane at high pressure, the membrane

acts as a ‘filter’ to selectively allow only some species to permeate to the downstream side to produce a specific component rich permeate stream.

Membrane separation can occur under both wet and dry conditions depending on what substances are being removed. The diffusion rate is dependent on partial pressure, membrane thickness and the chemical solubility of the substance. There is low and high pressure separation, gas-gas and gas-liquid separation [15].

Monsanto installed the first large-scale membrane systems (polysulfone) for hydrogen recovery from ammonia purge gas and refinery tail gas streams in the early 1980’s. Air separation systems to produce 95-99% N<sub>2</sub> were introduced in the late 1980’s. These systems produce N<sub>2</sub> for inerting fuel tanks, controlled atmosphere packaging for produce, and many other applications. Membranes are also used for natural gas and biogas purification (CO<sub>2</sub>, H<sub>2</sub>O, H<sub>2</sub>S removal), mainly with cellulose acetate polymers. However, these materials only have CO<sub>2</sub>/CH<sub>4</sub> selectivities of 12 to 15 under typical operating conditions [18], well below the low-pressure mixed gas selectivity of ~ 30 for dense membranes with zero permeate pressure [3]. Much of the decline in performance is due to plasticization of the membrane by CO<sub>2</sub> and heavy hydrocarbons.

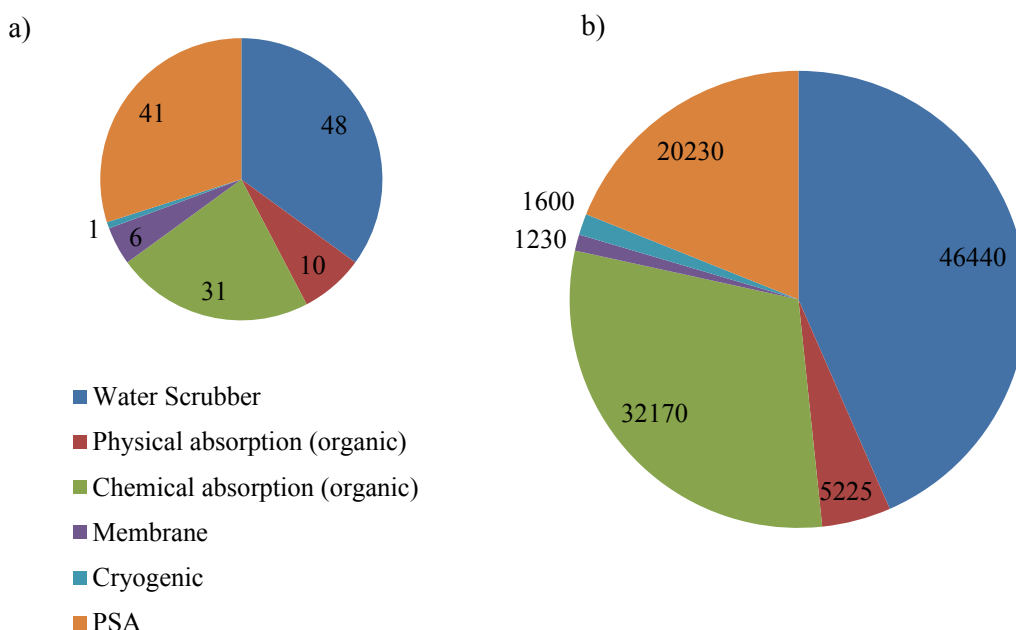


Figure 2.2. Biogas upgrading systems in Europe (a) number; (b) overall capacity [12].

Figure 2.2., shows the number of a particular type of biogas upgrading system (a) and the overall capacity of these systems (b) in the European context [12]. Membrane technology, despite being the cheapest to install and maintain [2], is not quite as popular as other systems. Amine absorption

processes dominate the acid gas removal market, but membranes would be preferable in many cases if they can maintain good performance in the presence of aggressive feed streams [1]. The development of stable membranes with high CO<sub>2</sub>/CH<sub>4</sub> selectivities would significantly enhance the competitive position of membranes relative to alternate technologies [18]. As of today, in commercial applications of membrane-based CO<sub>2</sub>/CH<sub>4</sub> separations, cellulose acetate polymers are most commonly used.

In membrane based biogas upgrading, permeability is an important factor where carbon dioxide and hydrogen sulphide can then pass through the membrane (fibre wall), while methane is retained. The upgrading process remains at high pressure, so no further compression is needed before addition to the gas grid [17, 15]. A shortcoming of membrane separation constitutes a conflict between high methane purity in the upgraded gas and high methane yield around 92% [15].

Operation at high permeate pressures is desirable from a CO<sub>2</sub> sequestration perspective, but it means that the average CO<sub>2</sub> concentration would be higher throughout the membrane, thus increasing the chances of plasticization. Moreover, as the CO<sub>2</sub> fraction in the feed increases, the membrane economics become more favourable, if the membrane performance remains stable.

These problems could be dealt with effectively by using mixed matrix membranes but it is still in a nascent phase of development from the viewpoint of large scale applications. Hence the scope of the present study will be restricted to mixed matrix membranes for biogas upgrading.

Mixed matrix membranes (MMM) have initially been produced in dense polymeric films for the purpose of gas transport facilitation through the membrane. The embedding of hydrophobic zeolites in rubber polymers proved to improve alcohol permeability and selectivity in pervaporation processes in the presence of water [19]. Similarly, MMM have been developed for gas separation processes in which different types of polymers and rigid filler materials were used. In this case the selectivity is achieved as a combination of the permeation rates of the desired gas through the polymer material and through the filler material. Initially, molecular sieves have been incorporated by dispersing zeolites in rubber polymers [20]. Also the dispersion of zeolites in glassy polymers has been studied [21, 22, 23, 80]. More recently, metal organic frameworks and carbon nanotubes have been used as dispersed material in the production of MMM for gas separation [24].

MMM materials combine the high selectivity of the filler materials with the low costs, manufacturing ease and flow behaviour of membranes [25]. MMM are characterized by high fluxes with low pressure drop, with a predominant convection-type of transport with the fillers acting like selective channels. By combining the properties of the polymer and filler, high permeabilities and selectivities can be achieved in membrane separation processes.



The flexibility in preparing different geometries tailored for specific applications is a great advantage of the MMM platform technology. An important factor for the MMM performance is the particle loading. The particle loading controls not only the capacity, but it also greatly influences the membrane forming process and the resulting structure. A main concern when producing MMM is to guarantee that the polymer, solvents and additives are compatible with the particles, so that the functionality will not be lost in the embedding process.

Usually, the main base material of an MMM is the polymer. Polymeric membranes are commonly classified into rubbery and glassy polymeric structures. These are defined by the temperature at which the amorphous polymeric material is used. When the amorphous polymeric material is operated above the polymer's glass transition temperature ( $T_g$ ), it is referred as a rubbery membrane. The  $T_g$  is a characteristic temperature which depends on the polymer structure and chemistry and is also of strong relevance to penetrant transport properties. Rubbery membranes can rearrange their structure on a significant time scale and are usually in thermodynamic equilibrium.

Usually, glassy polymers are operated below their  $T_g$  and actually never reach thermodynamic equilibrium because the time scale of polymer chain rearrangement is extraordinarily long. This non-equilibrated condition leads to the formation of micro-cavities within the polymer matrix due to the imperfectly packed polymer chains [26]. Glassy membranes have been studied widely in the literature and provide better performance for the selective layer, because the more restricted segmental motions in glassy polymers enhance 'mobility selectivity' compared to rubbery membranes [27, 28].

Polyimides are selected as the membrane material to be studied in this thesis. The term 'polyimides' refers to heterochain polymers containing an imide group in the backbone. The branched configuration inherent to the polyimide functional group allows many ring structures to be included in the polymer backbone [29]. These ring structures make the backbone chains stiff and result in a very narrow free-volume distribution [30]. In general, these polymers exhibit very high glass transition temperatures (in the range of  $\sim 300 - 424$  °C [30, 31]). This class of polymers has been studied extensively over the past 60 years, due to their high thermal and chemical stability and excellent physico-mechanical properties in a broad temperature range, in areas of electronics, electrical engineering, aviation and membrane separation [30]. Polyimides have found considerable industrial demonstration and significant commercial use by NKK Corporation Japan, Nitto Electric Co., Du Pont and Ube Industries, in membrane separation areas including ultrafiltration, reverse osmosis, hydrogen separation and recovery, helium purification and recovery, vapor separation and recovery and  $\text{CO}_2$  and acid gas separation [32]. The present work mainly focuses on the non-fluorinated polyimide, poly(3,3'-4,4'-benzophenone tetracarboxylic - dianhydride diaminophenylindane) (Figure 2.3), DTDA-DAPI. This is a commercially available polyimide with

a trade name of Matrimid<sup>®</sup> 5218 (Figure 2.3) and a glass transition temperature of 313 °C [33]. It exhibits a combination of selectivity and permeability for industrially significant gas pairs (e.g. CO<sub>2</sub>/CH<sub>4</sub> and CO<sub>2</sub>/N<sub>2</sub>) superior to other readily available polymers [34].

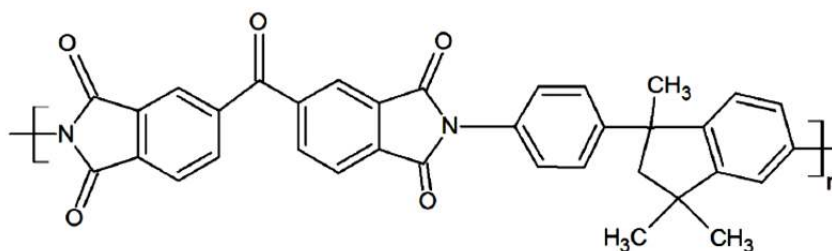


Figure 2. 3. Structure of Matrimid<sup>®</sup>5218

From the perspective of CO<sub>2</sub> removal from a gas stream using a membrane based method probably the most successful additive could be considered to be ionic liquids. Ionic liquids (IL) are defined as the liquids which solely consist of ions (cations and anions), as opposed to an ionic solution, which is a solution of a salt in a molecular solvent and have a melting point of 100 °C or below. ILs which are liquid at room temperature are called room temperature ionic liquid (RTIL). Ionic liquids have gained great attention in a variety of chemical processes due to their unique properties such as non-volatility, non-flammability, high thermal stability and nature of tailoring physical properties by selection of different cations and anions, and so on [35]. A potential application of ionic liquids is for gas separation processes e.g. post combustion CO<sub>2</sub> capture from power plants and CO<sub>2</sub> removal from natural gas/biogas etc. The non-volatile nature of ionic liquids would not cause any contamination to a gas stream, and thus this feature gives ionic liquids a big advantage over conventional solvents used for absorbing gases. To select an efficient ionic liquid for use as a gas separation medium, it is necessary to know the solubility of the gas in the ionic liquid phase. Reliable information on the solubility of gases in ILs is needed for the design and operation of any possible processes involving IL [36].

Various experimental studies on gas separation processes using ionic liquids have been conducted by researchers and are available in literature. A number of investigations have shown that CO<sub>2</sub> is remarkably soluble in several ILs. Figure 2.4 above shows two such popular ILs which have been used for CO<sub>2</sub> capture.

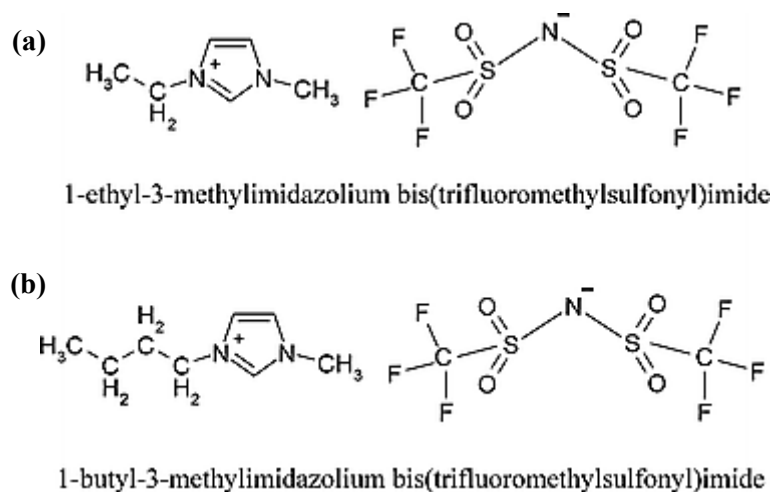


Figure 2.4. Chemical structure of (a) [emim][Tf<sub>2</sub>N] and (b) [bmim][Tf<sub>2</sub>N]

Solubility measurements [7, 37], spectroscopic studies [38], and molecular simulations [7] indicate that CO<sub>2</sub> solubility in ILs depends primarily on the strength of interaction of CO<sub>2</sub> with the anion. Cadena et al., [7] studied the mechanism of CO<sub>2</sub> dissolution in imidazolium type ILs by experimental and molecular modeling and found that the anions have larger impact on the solubility of CO<sub>2</sub>. Anthony and co-workers made a comparison between different ionic liquids with same cation and different anions to see their affinity to absorb CO<sub>2</sub>. They used three ionic liquids with same cation i.e. 1-butyl-3-methylimidazolium ([bmim]) and three different anions i.e. tetrafluoroborate ([BF<sub>4</sub>]), hexafluorophosphate ([PF<sub>6</sub>]), bis(trifluoromethylsulfonyl)imide ([Tf<sub>2</sub>N]) to check the effect of anion on CO<sub>2</sub> solubility. The results showed that the CO<sub>2</sub> solubility is dependent on the choice of the anion [6]. The ionic liquid with the [Tf<sub>2</sub>N] anion has a considerably higher affinity for CO<sub>2</sub> than either of the other two ionic liquids. The [bmim][BF<sub>4</sub>] and [bmim][PF<sub>6</sub>] have basically the same solubility, although the [bmim][PF<sub>6</sub>] appears more soluble at higher pressures. The solubility of CO<sub>2</sub> in [bmim][Tf<sub>2</sub>N] at different temperatures was also measured which showed that the solubility decreases with increase in temperature and increases with increase in pressure [39]. Lee et al., [40] measured the CO<sub>2</sub> solubility in [bmim][Tf<sub>2</sub>N] at different temperatures and pressures. The solubility data measured is compared with the data reported by Anthony et al., [39]. The two sets of data were measured at slightly different temperatures. The results showed that the two sets of solubility data are in good agreement qualitatively. At low pressures, the gas solubilities appear linear as a function of the pressure but exhibited a nonlinear trend as the pressure increased, at all four different temperatures [40].

Popularly, there are three systems which have been used for CO<sub>2</sub> capture using ionic liquids. Absorption system (absorber and stripper) is one of the most common techniques for gas purification in which the flue gas is bubbled through the solvent (e.g. ionic liquid), the solvent will absorb the gas of interest (e.g. CO<sub>2</sub>) from flue gas and the solvent is then regenerated in the stripper to use it

again in the system [41]. The main disadvantage of this system is the large quantity of ionic liquid required and the possible toxicity/environmental impact of the same.

Supported ionic liquid membranes (SILM) are the second technique that can be used for CO<sub>2</sub> capture medium using ionic liquids. In SILM system, just the pores of a membrane are filled with the solvent (e.g. ionic liquid). The more soluble gas is able to permeate across the membrane, while the less soluble gas remains on the feed side. The flux of the gas across the membrane is affected by the thickness of the membrane. A thinner membrane yields a higher flux, but the thinner the layer of solvent, the quicker the solvent evaporates. But, due to non-volatile nature of ionic liquids this problem can be eliminated in case of ionic liquids - SLM systems [42]. The limiting factor, inhibiting the use of SILM is membrane instability at higher pressures wherein there is the tendency of the ionic liquid to “leak” out of the membrane system into the product or feed stream. In order to circumvent this problem there have been some studies carried out to make membranes with ILs in the form of polymeric room temperature ionic liquid and ionic liquid gels. In a recent study, Hao et al.[43], report very high performance in terms of permeability and selectivity for a membrane synthesized using [vbim][Tf<sub>2</sub>N]/[emim][B(CN)<sub>4</sub>] and the filler metal organic network - ZIF8. However, their mechanical and thermal stability is still not up to par with polymers.

In the third type of system the ionic liquid is incorporated in the membrane, possibly cross linked into the dense matrix of the membrane. This type of system offers the advantage of SILM overcoming the common disadvantages detailed above. In most cases it is found that due to the incorporation of the ionic liquid, the properties of the base polymer in terms of permeability and selectivity to a particular feed component and thermal and mechanical stability are enhanced. To make such a system the polymerization process and environment have to be tweaked i.e., choosing the right solvent and polymer is very crucial.

As discussed previously, inorganic fillers form a very crucial part of a mixed matrix membrane. One such class of compounds which have recently become the focus of research are Metal Organic Frameworks (MOFs). MOFs are crystalline compounds which consist of a metal ion or clusters which are bound by coordinated bonds to rigid organic molecules. These organic molecules act as linkers to the metal ions. The properties of the MOF depend on the choice of the metal and the linker. They form one-, two-, or three- dimensional structures, and are porous in nature. These are having unique properties, such as highly diversified structure, large range in pore sizes, high surface areas, and specific adsorption affinity. Structures of some popular MOFs are shown below in Figure 2.5.

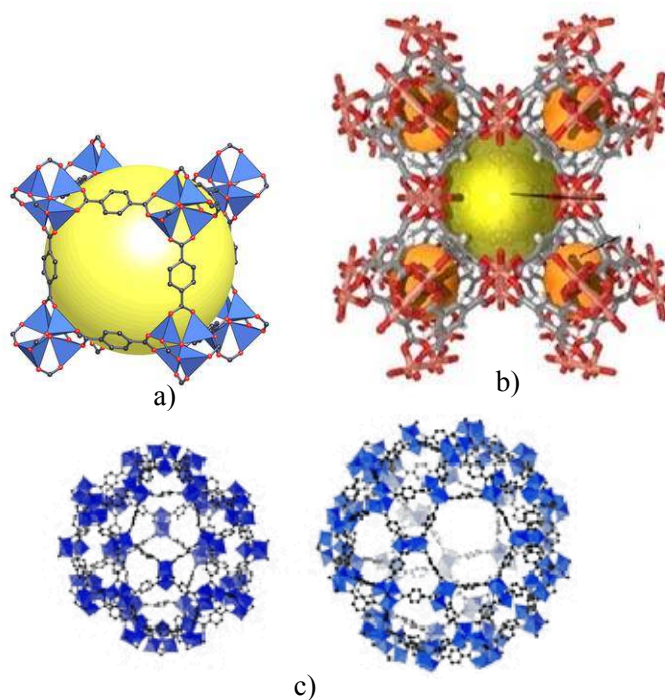


**Figure. 2. 5. Structural representation of (a) MOF 5 (b) Cu<sub>3</sub>(BTC)<sub>2</sub> and (c) MIL 101**

Usually MOFs are prepared under solvo-thermal or hydrothermal conditions. In this method substances are crystallized from high temperature aqueous solutions at high vapour pressure. This type of synthesis depends on the solubility of minerals in hot water under high pressure. Crystal growth is performed in autoclave to provide high vapour pressure. The reactants are supplied in it along with water. A temperature gradient is maintained at the opposite ends of the chamber. So, the hotter end dissolves the reactants and the cooler end causes the seed crystals to grow. The table below shows a list of popular mixed matrix membranes made with MOFs with some important parameters which characterize their performance.

Table. 2. 2. Details about some popular MOFs which are being researched worldwide.

MOF	Polymer	Loading		PCO <sub>2</sub>	αCO <sub>2</sub> /CH <sub>4</sub>	Commerci al name	References
		%	Gases				
		(wt/wt)					
<b>Cu-MOF</b>	-	-	CO <sub>2</sub> /CH <sub>4</sub>	-	26	-	44
<b>Cu<sub>3</sub>(BTC)<sub>2</sub> (HKUST 1)</b>	Matrimid	30	CO <sub>2</sub> /CH <sub>4</sub>	1-1.5 [GPU]	20-30	<a href="#">Basolite</a> <a href="#">C300</a>	4,5
<b>ZIF 8</b>	Matrimid	30	CO <sub>2</sub> /CH <sub>4</sub>	9.5[barrer]	43.6	<a href="#">Basolite</a> <a href="#">Z1200</a>	4,45,46
<b>MIL 53</b>	Matrimid	30	CO <sub>2</sub> /CH <sub>4</sub>	1.4 [GPU]	29-30	<a href="#">Basolite</a> <a href="#">A100</a>	4,47
<b>ZIF 69</b>	Alumina	-	CO <sub>2</sub> /CH <sub>4</sub>	103.4 [10 <sup>-9</sup> mol m <sup>-2</sup> s <sup>-1</sup> Pa <sup>-1</sup> ]	6.3	-	48,49
<b>ZIF 7</b>	Pebax/PTSM P/alumina	34	CO <sub>2</sub> /CH <sub>4</sub>	41 [barrer]	44	-	50,51
<b>Cu TPA</b>	PVA	15	CO <sub>2</sub> /CH <sub>4</sub>	2.44 [barrer]	40.4	-	52
<b>MOF 5</b>	Matrimid/al umina	30	CO <sub>2</sub> /CH <sub>4</sub>	20.2 [barrer]	44.7		53,54,55
<b>Cu-BPY-HFS</b>	Matrimid	30	CO <sub>2</sub> /CH <sub>4</sub>	15.06 [barrer]	25.55	-	56
<b>ZIF 90</b>	6FDA- DAM/MATRI MID	15	CO <sub>2</sub> /CH <sub>4</sub>	720/590 [barrer]	37/34	-	57
<b>Cu (HCOO)<sub>6</sub></b>	-	-	CO <sub>2</sub> /CH <sub>4</sub>	2.25*10 <sup>-6</sup> [mol/m <sup>2</sup> .s. Pa]	12.63	-	58
<b>NH<sub>2</sub>-MIL-53(AL)</b>	PSF	25	CO <sub>2</sub> /CH <sub>4</sub>	10 [barrer]	17	-	59
<b>AMIDE-MIL53</b>	6FO-DMF (polyimide)	25	CO <sub>2</sub> /CH <sub>4</sub>	15 [barrer]	66	-	60

\*1 GPU = 7.5005 x 10<sup>-16</sup> m<sup>2</sup>·s<sup>-1</sup>·Pa<sup>-1</sup>

\*\*1 Barrer = 7.5005 x 10<sup>-18</sup> m<sup>2</sup>·s<sup>-1</sup>·Pa<sup>-1</sup>

Many potential uses of MOFs include gas purification, gas storage, gas separation and heterogeneous catalysis [56]. Because of strong chemisorption that takes place between electron rich, odour-generating molecules and the framework that allows the desired gas to pass through it, MOFs are promising for gas purification. These can store molecules such as carbon dioxide, carbon monoxide, methane, and oxygen due to their high adsorption enthalpies. Gas separation can be performed as they can allow certain molecules to pass through their pores based on size and kinetic diameter. These can be used as catalysts because of their shape and size selectivity. Because of their very porous structure, mass transport in the pores is not hindered. MOF as membrane material can be used mainly for continuous membrane-based separations, membrane reactors etc. Along with their various applications, many significant drawbacks are attached with MOFs. These are mechanically and chemically unstable, due to their nature of bonding. Some of them are prone to the formation of cracks and fractures and are extremely sensitive to moisture. Despite extensive research, there still exist some challenges to fabricate low cost, crack free, continuous MOF based membrane.

## ***2.4. Economics of biogas upgrading***

Economics is an important factor in determining if a particular technology is feasible and profitable for an industry. Analysis of cost to gains has been performed for biogas production and upgrading in the European context by several industries and commissions appointed by the EU. According to Urban [16] the investment costs for a biogas upgrading plant treating 500 Nm<sup>3</sup> biogas/h are on the average €1,000,000 while for a plant treating 2,000 Nm<sup>3</sup> biogas/h the investment costs are close to €3,000,000. Investment costs (€/Nm<sup>3</sup> biogas) decrease as size of the plant increases; for a plant treating 2,000 Nm<sup>3</sup> biogas/h the costs are €1,500 /Nm<sup>3</sup> and for a plant treating 500 Nm<sup>3</sup> biogas / h the costs are on average €2,300 /Nm<sup>3</sup> (Table 2.3.) De Hullu et al. [62] predicts service/maintenance costs of around €50,000 annually including one annual internal and external inspection of the plant. Urban [16] estimates that the maintenance costs are around 2 % of the predicted capital costs and the water costs are assumed to be around €2 /m<sup>3</sup>

De Hullu et al. [62] does not mention scale but chemical absorption investment costs for carbon dioxide and hydrogen sulphide removal are €869,000, PSA the cost is around €680,000, cryogenics is the most expensive option and the cheapest is membrane separation wherein the cost is €233,000.

**Table 2.3. Biogas upgrading plants operating equipment from the manufacturers [62]**

	Water Scrubbing	PSA	Chemical Scrubbing	Membrane Separation	Cryogenic
Investment cost (€/year)	€ 265,000	€ 680,000	€ 353,000 - 179,500	€ 233,000 – 749,000	€ 908,500
Maintenance cost (€/year)	€ 100,000	€ 187,250	€ 134,000 - 179,500	€ 81,750 – 126,000	€397,500
Cost per Nm <sup>3</sup> /biogas upgraded	€ 0.13	€ 0.25	€ 0.17 – 0.28	€ 0.12 – 0.22	€ 0.44

De Hullu et al. [62] predicts the operational costs for chemical absorption for carbon dioxide and hydrogen sulphide removal €179,500 annually, high pressure water scrubbing costs were €110,000 and PSA operational cost is €187,250. Cryogenics operational cost is €397,500 and membrane separation is €81,700.

**Table 2.4. Comparison of demands for the most common technologies at large and small scale [63]**

	Water Scrubbing	Catalytic Absorption	PSA	Membrane Separation	Cryogenics	Large Scale	Small Scale
Gas quality	High	High	High	High	High	High	High
Gas Quantity Volume	High	High	Medium	Low	Medium	High	Low
Compact	Medium	Medium	No	Yes	No	Medium	Yes
Methane Efficiency	High	High	Medium	Low	High	High	Low
Emissions	Low	Low	Medium	Medium	Low	Low	Medium
Waste Streams	Continuous	Continuous	Batch	Batch	Continuous	Continuous	Batch

Green best for Small Scale, Yellow best for Large Scale, Blue for Both.



Urban [16] stated that the substrate cost had a large influence on the cost of biogas production and when the substrate prices are over €35 /tonne it can result in plants having a low income or even a negative income.

The operating cost for biogas upgrading plants decreases as the size of the facilities increase. Operating costs for a plant of around 500 Nm<sup>3</sup> biogas / h are on average €220, 000 /y. As the investment costs, also the operating costs per Nm<sup>3</sup>of biogas will be lower in larger upgrading units (Table 2.4). Operating costs for a plant treating 500 Nm<sup>3</sup> biogas / h are €440/Nm<sup>3</sup> while for a plant treating 2,000 Nm<sup>3</sup> biogas / h the cost are about €340/Nm<sup>3</sup> [16, 17].

Membrane technology, despite being the cheapest to install and maintain [2], is not quite as popular as other systems. The development of stable membranes with high CO<sub>2</sub>/CH<sub>4</sub> selectivities would significantly enhance the competitive position of membranes relative to alternate technologies.

Based on this premise, in the present study, we attempt to develop ionic liquid incorporated dense Matrimid membranes. In such membranes the ionic liquid is impregnated inside a dense membrane by a physico - chemical interaction like cross-linking achieved by careful selection of polymerization environment i.e., the solvent and physical conditions [11]. In most cases such membranes exhibit properties which are midway between SILMs and dense gas separation membranes. They also show improved mechanical and thermal properties in comparison to the former. Furthering these concepts, efforts have also been made to develop ionic liquid incorporated mixed matrix membrane with dispersed MOF particles with the potential objective of using it for high performance biogas upgrading.

---

## 3. MATERIALS AND METHODS

---

### 3.1. Membrane preparation

Matrimid<sup>®</sup> 5218 was obtained from Huntsman USA. Three custom synthesized MOFs were obtained from our collaborators in the University of Porto - MOF-5, MIL101 and [Cu<sub>3</sub>(BTC)<sub>2</sub>]. The ionic liquid, 1-butyl-3-methylimidazolium bis(trifluoromethanesulfonyl) imide, more commonly known as [bmim][Tf<sub>2</sub>N] was acquired from IoLiTec Ionic liquid technologies GmbH, Germany.

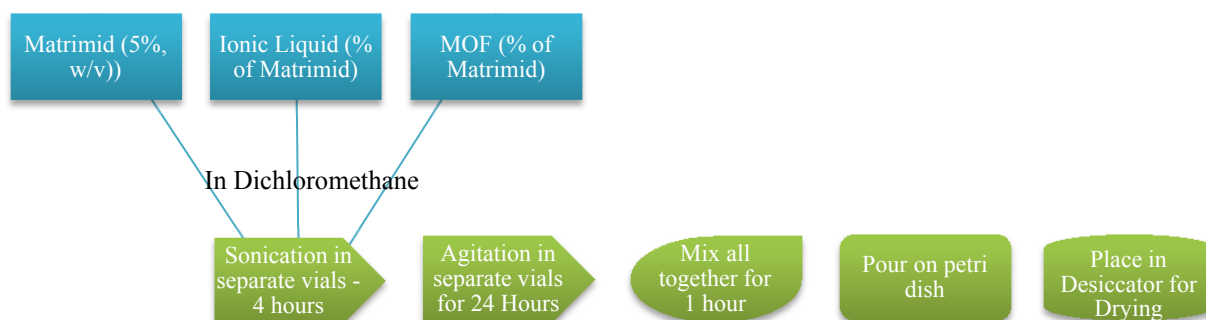


**Figure 3. 1. Scheme of method of membrane preparation**

Figure 3.1 shows a schematic representation of the membrane making process. The membranes were prepared by the method of solvent evaporation. 5% w/v solutions of Matrimid were prepared in 20ml glass vials by dissolving 0.5g Matrimid in 4.5 ml of dichloromethane. The additive solutions (ionic liquid and/or MOF) were prepared in separate 20ml vials in dichloromethane. The additive loading was determined by the following equation [4] (Eq. 3.1):

$$\% \text{ Loading (wt\%)} = \frac{\text{Weight of additive}}{\sum(\text{Weight of additives}) + \text{Weight of matrimid}} \times 100 \dots \dots (\text{Eq. 3.1})$$

The volume of ionic liquid required to make solutions of varied concentrations were calculated on the basis of the density of the ionic liquid. The solutions were sonicated for 4 hours and agitated for 24 hours separately on magnetic stirrers [2]. They were then mixed and agitated for 1 hour before pouring them into flat bottomed petri dish and kept in desiccators for drying. Table 3.1., shows an example of the component quantities to make neat Matrimid, 50% IL loaded and 50% IL with 20% MOF loaded membranes.

Table 3. 1. Example of the quantities of components added to make the membranes

Vial	Component/Membrane	Neat Matrimid	Matrimid with 50% IL	Matrimid with 50% IL and 20% MOF
1	Matrimid	0.5g in 9.5 ml dichloromethane	0.5g in 4.5 ml dichloromethane	0.5g in 4.5 ml dichloromethane
2	Ionic Liquid	0	0.25g in 5 ml dichloromethane	0.25g in 2.5 ml dichloromethane
3	MOF	0	0	0.1g in 2.5ml dichloromethane

### 3.2. Contact Angle

The contact angle ( $\theta$ ) of a liquid drop on a solid surface is defined by the mechanical equilibrium of the drop under the action of three interfacial tensions: solid-vapour ( $\gamma_{SV}$ ), solid-liquid ( $\gamma_{SL}$ ) and liquid-vapour ( $\gamma_{LV}$ ) (Figure 3.2).

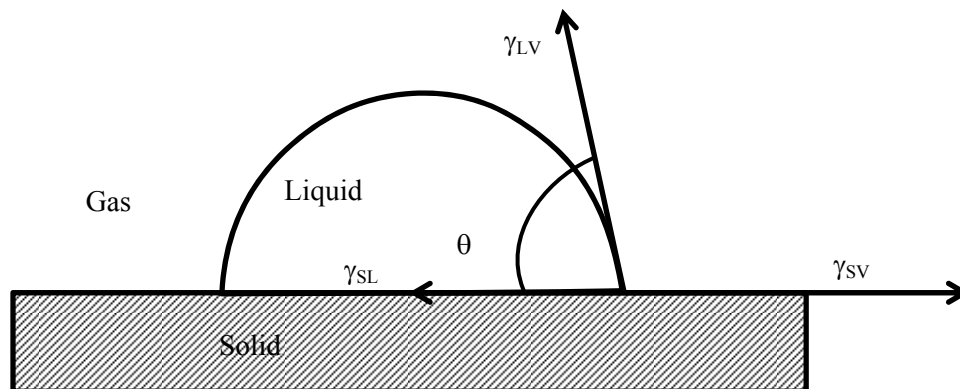


Figure 3. 2. Schematic of a sessile drop, contact angle and the three interfacial tensions are shown [64].

The equilibrium spreading coefficient ( $W_s$ ) is defined by equation and can only be negative or zero (Eq. 3.2.1):

$$W_s = W_a - W_c = \gamma_{SV} - \gamma_{LV} - \gamma_{SL} \dots \dots (Eq. 3.2.1)$$

Where  $W_a$  and  $W_c$  are the work of adhesion and work of cohesion respectively and can be defined as

$$W_a = \gamma_{LV} + \gamma_{SV} - \gamma_{SL} \dots \dots (Eq. 3.2.1)$$

$$W_c = 2 \cdot \gamma_{LV} \dots \dots (Eq. 3.2.1)$$

The contact angle ( $\theta$ ) was measured by sessile drop method. A drop of distilled water is deposited manually on the membrane surface by a Pasteur pipette. Various photographs are acquired by the software and the tangent is determined by fitting the drop shape to known mathematical functions. The measurements are performed immediately after the drop falls on the surface. Multiple replicates are performed and the mean contact angle is reported with its standard deviation.

### **3.3. Scanning Electron Microscopy (SEM)**

The surface structure of the mixed matrix membranes prepared were analysed by the means of a Jeol JSM-7001 F – Field emission scanning electron microscope, operated with an electron beam intensity of 10kV. This microscope allows for the observation and characterization of heterogeneous organic and inorganic materials at the scale of micro ( $10^{-6}$ ) to nano ( $10^{-9}$ ) meters. Cross section imaging also can be done by using the “tilt” facility which allows the sample to be held at an angle of  $45^\circ$  for analysis.

The principle of SEM involves the incidence of an electron beam on the sample surface producing secondary electrons, backscattered electrons or retro-diffused x-rays which can be analysed to obtain an image which is magnified over 200,000 times. In our case, the signal consists of secondary electrons from which the surface image is constructed instantly. The primary electron beam is mobile and scans the sample surface obtaining a complete image.

Sample preparation is an important part of this process as the material has to be clean cut surfaces and must be a good conductor. In order to achieve this,  $2 \text{ cm}^2$  pieces of the sample were cut in a liquid nitrogen environment to avoid distorting the material surface or cross section. The sample is then impregnated with a thin layer of gold particles to make it a good conductor.

### **3.4. Mechanical Properties**

Puncture tests were carried out using a TA-XT plus texture analyser (Stable Micro Systems, Surrey, England). All mechanical tests were performed at ambient conditions. Three replicates of each film were analysed.

#### **3.4.1. Puncture test**

Puncture tests were carried out by immobilizing the test samples (30x30 mm) on a specially designed base with a hole of about 10 mm diameter. The samples were compressed at a speed of 1mm/s and punctured through the hole with a cylindrical probe (2mm diameter). The puncture stress

( $\sigma_p$ ) was expressed as the ratio of the puncture strength by the probe contact area as per equation below (Eq 3.4.1).

$$\sigma_p = \frac{F_p}{S_p} \dots \dots (Eq. 3.4.1)$$

Where  $\sigma_p$  is the puncture stress (in Pa);  $F_p$  is the force to the films (in N); and  $S_p$  is the probe cross sectional area (in m<sup>2</sup>).

This test allows the determination of the strain by equation (Eq. 3.4.2)

$$\varepsilon = \frac{L_f - L_i}{L_i} \times 100 \dots \dots (Eq. 3.4.2)$$

Where  $\varepsilon_p$  is the puncture elongation;  $L_f$  is the final length (in m); and  $L_i$  is the initial length (in m).

The parameter  $L_f$  refers to the film elongation and it is calculated with base in the elongation measured by the probe,  $d$  (Eq. 3.4.3). The Figure 3.3., below shows a representation of the test calculation.

$$L_f^2 = d^2 + L_i^2 \leftrightarrow L_f = \sqrt{d^2 + L_i^2} \dots \dots (Eq. 3.4.3)$$

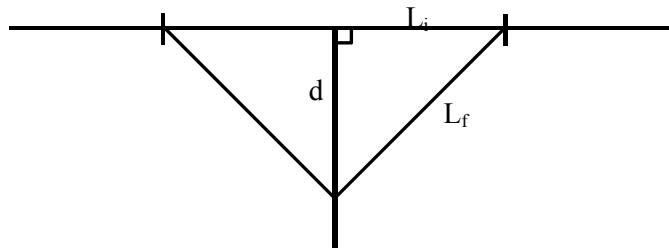
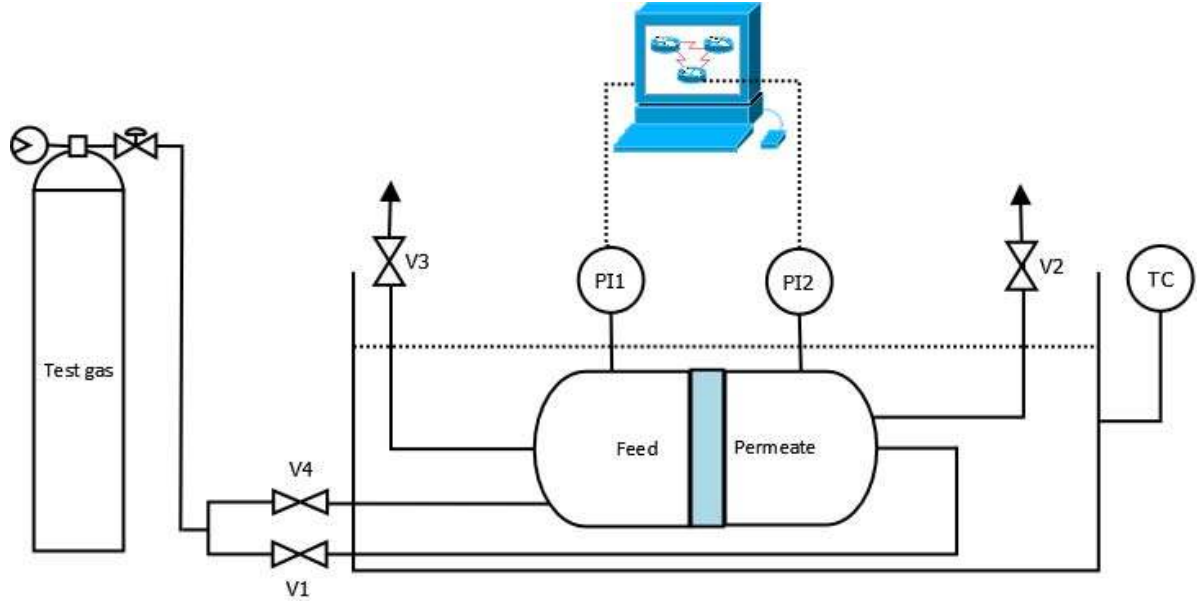


Figure 3.3. Puncture Test Scheme

### 3.5. Gas Permeability

To find the permeability of the membrane samples were cut into 2 cm diameter discs and their thickness was measured using a micro-meter screw gauge (Braive Instruments, USA). The experimental apparatus is composed of a stainless steel cell with two identical chambers separated by the test sample. The permeability was evaluated by pressurizing one of the chambers (feed) up to 700 mbar, with pure methane or carbon dioxide followed by the measurement of the pressure change

in both chambers over time, using two pressure transducers. The measurements were made at constant temperature of 30 °C ensured by immersing the cell in a thermostatic water bath (Julabo, Model EH, Germany) as shown in the picture below.



**Figure. 3. 4. Gas permeation setup; V1, V4 are inlet valves; V2, V3 are exhaust valves; PI1, PI2 are the pressure transducers. The whole setup is placed in a thermostatic water bath.**

The permeability was calculated by the method described by Cussler et al.,[65], with the pressure data obtained from both compartments and by the software LabView and MS Excel by the following equation (Eq 3.5.1):

$$\frac{1}{\beta} \ln \left( \frac{[p_f - p_p]_0}{[p_f - p_p]} \right) = \frac{1}{\beta} \ln \left( \frac{\Delta p_0}{\Delta p} \right) = P \frac{t}{\delta} \dots \dots (Eq. 3.5.1)$$

Where  $p_f$  and  $p_p$  are the recorded pressures in the feed and permeate compartments respectively;  $P$  is the gas permeability;  $t$  is the time;  $\delta$  is the membrane thickness and  $\beta$  is a constant called the geometric parameter which is calculated for a given system by the following equation (Eq. 3.5.2):

$$\beta = A \left( \frac{1}{V_f} + \frac{1}{V_p} \right) \dots \dots (Eq. 3.5.2)$$

Where  $V_f$  and  $V_p$  are the volumes of the feed and the permeate compartment respectively and  $A$  is the membrane area. This parameter is calculated with a PDMS membrane and nitrogen as the test gas using the reported permeability value of standard PDMS available,  $P_{N_2/PDMS} = 2.3 \times 10^{-10} \text{ m}^2\text{s}^{-1}$ . The membrane gas permeability is obtained by the slope represented by the curve between  $(1/\beta)\ln(\Delta p_0/\Delta p)$  and  $t/\delta$ .

---

## 4. RESULTS AND DISCUSSION

---



## **4.1. Membrane Preparation**

Matrimid is soluble and polymerizes (on drying) in several organic solvents like dichloromethane, THF, chloroform, etc., as reported in literature. However to obtain ionic liquid cross linked membranes with Matrimid is slightly challenging. In the present work we experimented with two different solvents – chloroform and dichloromethane. With chloroform it was observed that when the ionic liquid concentration exceeded 15% (wt./wt. of Matrimid) a very porous membrane was obtained after drying with ionic liquid residue remaining behind in the petri dish. However, with dichloromethane stable dense membranes were obtained even with 90% ionic liquid (wt./wt. of Matrimid) loading. It is unclear and beyond the scope of this study, whether this is the case only with the ionic liquid used herein i.e., [bmim][Tf<sub>2</sub>N], or is a general phenomenon.

It was also interesting to observe that membranes prepared in the glass petri dishes, on drying in the desiccator, were rigidly attached to the glass when ionic liquid concentration greater than 40% (wt./wt. of Matrimid) was used. Hence Teflon plates were used to prepare membranes with higher ionic liquid loading.

The membranes obtained after complete drying were homogeneous and flexible. The membrane thickness varied from 70µm to 400µm based on the amount of ionic liquid added. The membrane thickness increased with increased loading of ionic liquid. The Matrimid control membrane is yellow in colour and completely transparent. As the ionic liquid loading was increased the membrane became more opaque and flexible. On addition of MOFs the membrane acquired varied colouration depending on the MOF used – green for MIL101, light blue for Cu<sub>3</sub>(BTC)<sub>2</sub> and whitish-yellow for MOF 5. Attempts were made to synthesize membranes with loading of 80% IL and 20% MOF but it led to gel-like precursors and formation of defective membranes. Thus based on other characteristics studied it was decided to proceed with membranes which are loaded with 50% IL and 20% MOF. These membranes were successfully synthesized.

## **4.2. Surface Properties**

### **4.2.1. Contact Angle**

Surface properties of a membrane give information about its hydrophilicity. The contact angle increases with increasing surface hydrophobicity. This can help better understand the kinetic interaction of the gases with the membrane surface.

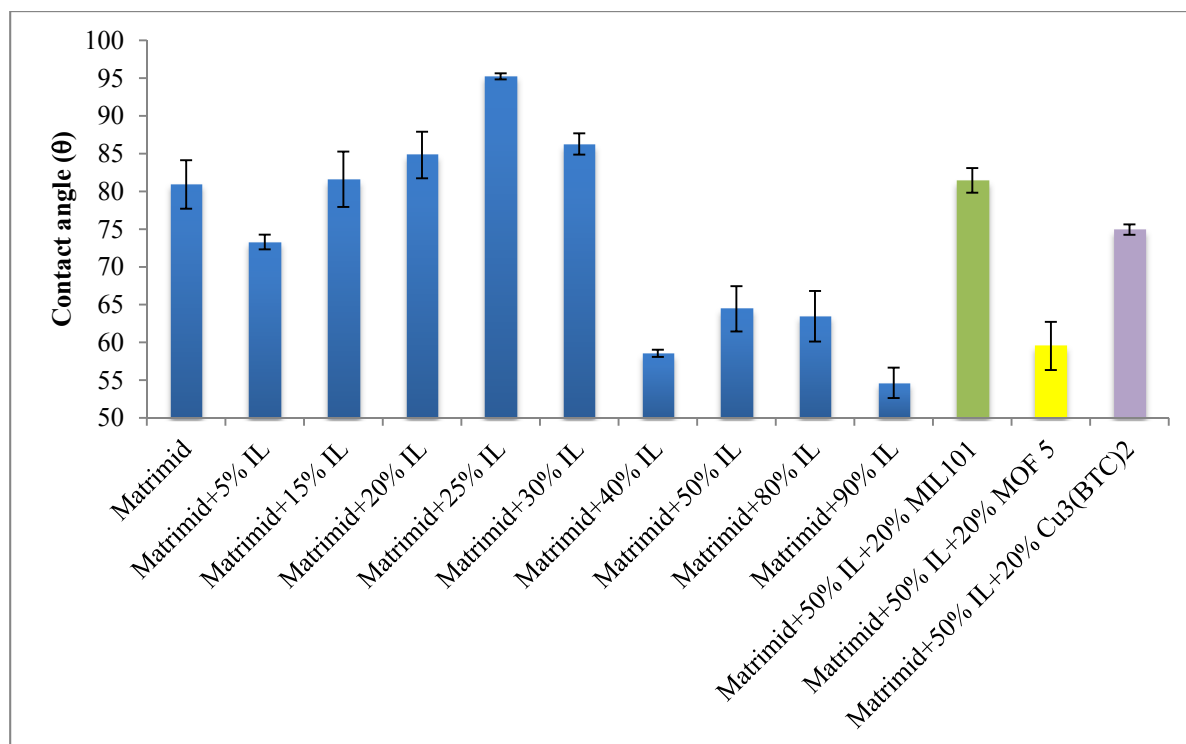


Figure 4. 1. Contact angle for membranes with different IL contents

Despite the errors it can be seen from Figure 4.1 that the contact angle increases with increase in ionic liquid % in the membrane till about 25% loading and then decreases. This means that the hydrophobicity of the membrane surface increases with increasing IL % until 25% loading and then the membrane becomes very hydrophilic. However, except for the membrane with 25% IL loading none of the membranes is hydrophobic. For neat matrimid (0% IL) the data is in corroboration with that reported in literature [20]. But it was contradictory for other samples as it was expected that the hydrophilicity would increase with increase in IL doping.

The interaction of a polar molecule like CO<sub>2</sub> with the membrane increases with increase in its hydrophilicity. Thus it could mean that CO<sub>2</sub> is more favourably adsorbed or permeated through the membrane. This also means that the membrane has low affinity for a non-polar molecule like CH<sub>4</sub>. Hence higher % IL could prove to be more feasible membranes for CO<sub>2</sub> separation from methane.

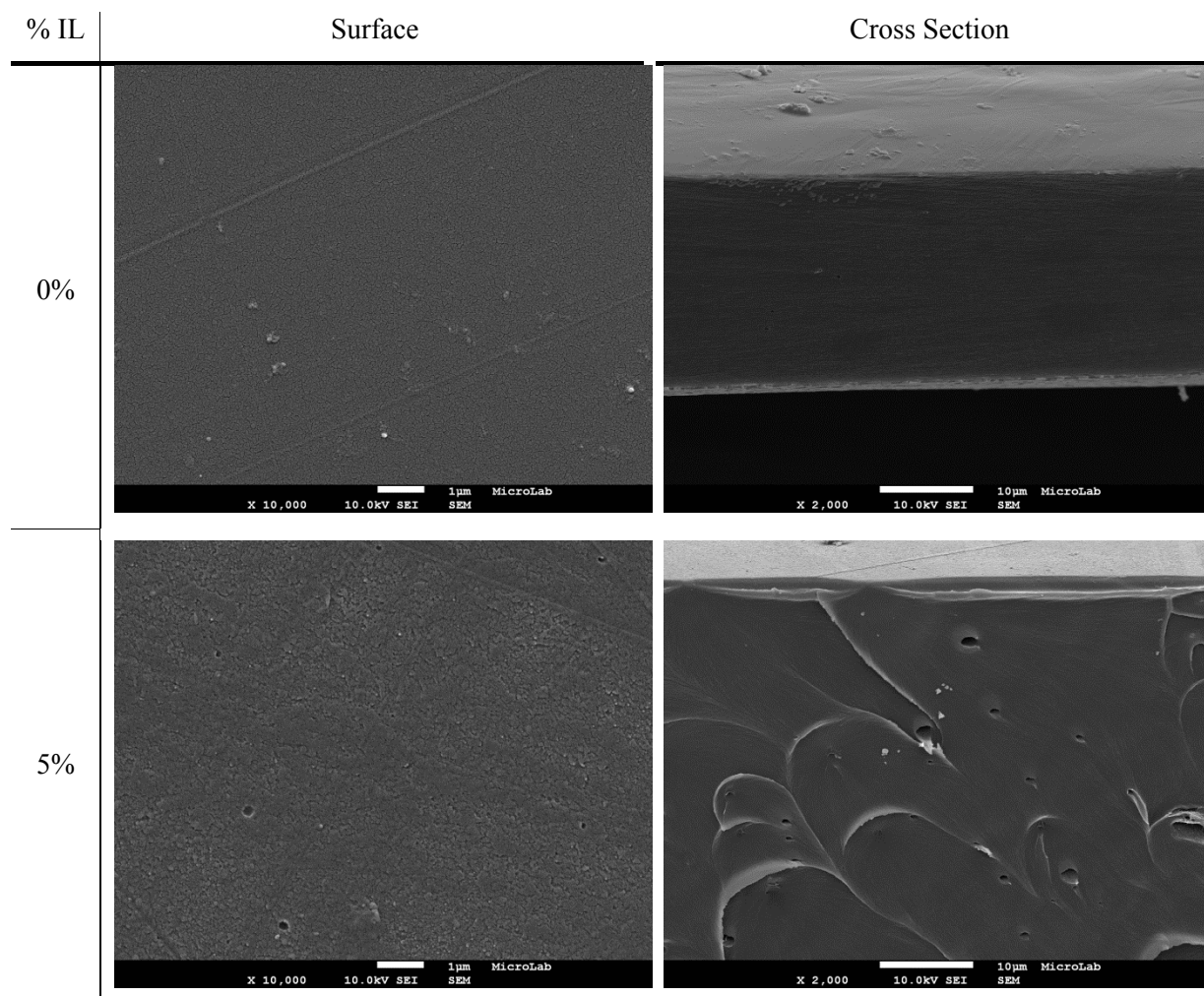
It is also interesting to note that addition of MOF particles augmenting with the IL significantly changes the hydrophilicity of the resulting membranes. In this case the membrane with MOF- 5 seems to have highest hydrophilicity compared to those with MIL 101 and Cu<sub>3</sub>(BTC)<sub>2</sub>.

It is important to note in this experiment that the associated gross error is significant since the measurement is heavily dependent on the visual prowess and experience of the instrument operator. In each trial several film samples and drops of fluid were used. The concluding result recorded was

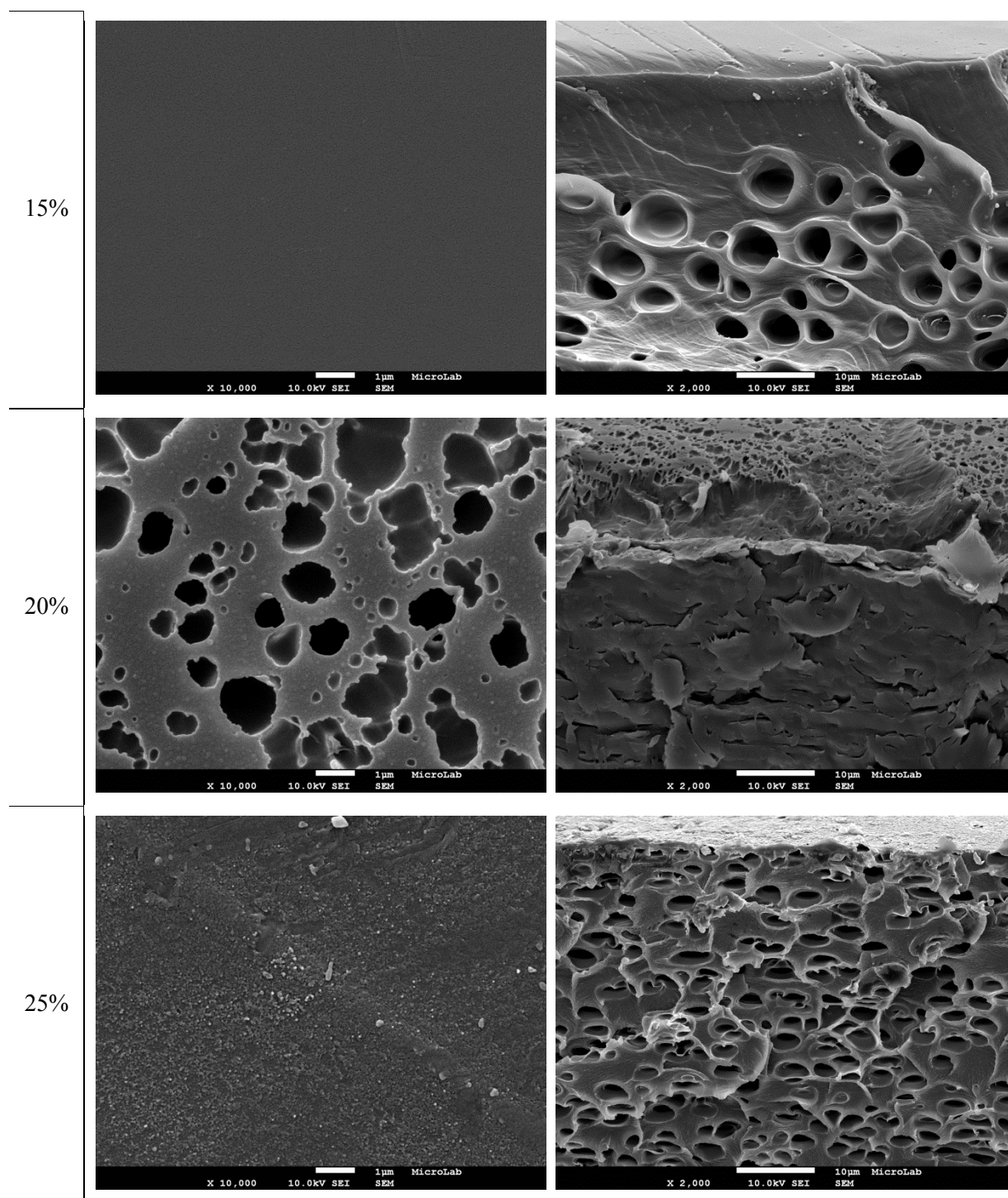
for the trial considered by the operator to be the best. For best results the contact angle recorded in the first 5 seconds was considered.

### 4.3. Scanning Electron Microscopy (SEM)

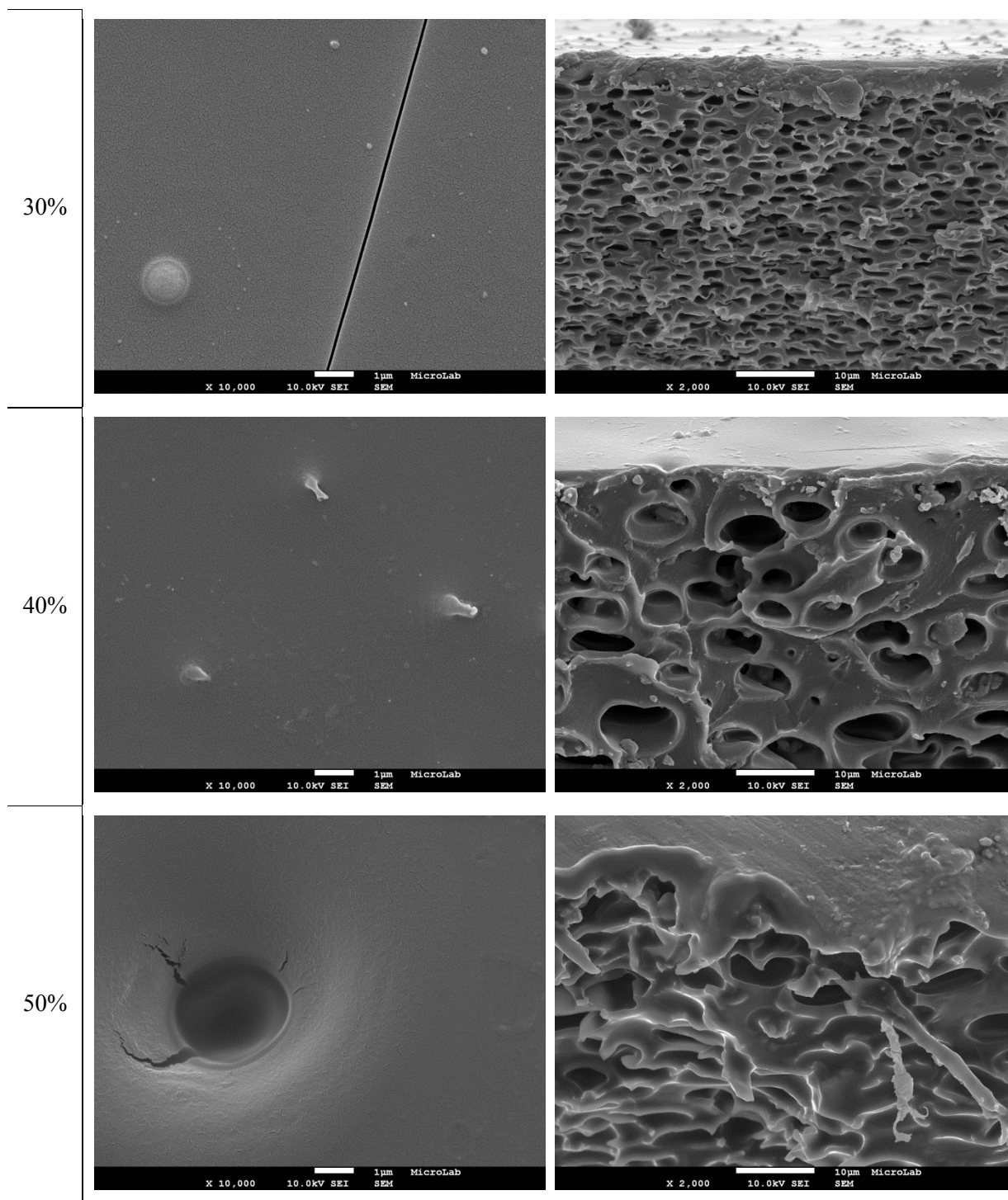
The scanning electron microscopy images depict the surface and cross section to better understand the structure of the mixed matrix membrane with increasing ionic liquid concentrations. The magnification used was 10000x for the surface and 2000x for the cross sectional view.



DEVELOPMENT OF MIXED MATRIX MEMBRANES WITH METAL – ORGANIC FRAMEWORKS AND IONIC LIQUIDS FOR BIOGAS UPGRADING



DEVELOPMENT OF MIXED MATRIX MEMBRANES WITH METAL – ORGANIC FRAMEWORKS AND IONIC LIQUIDS FOR BIOGAS UPGRADING



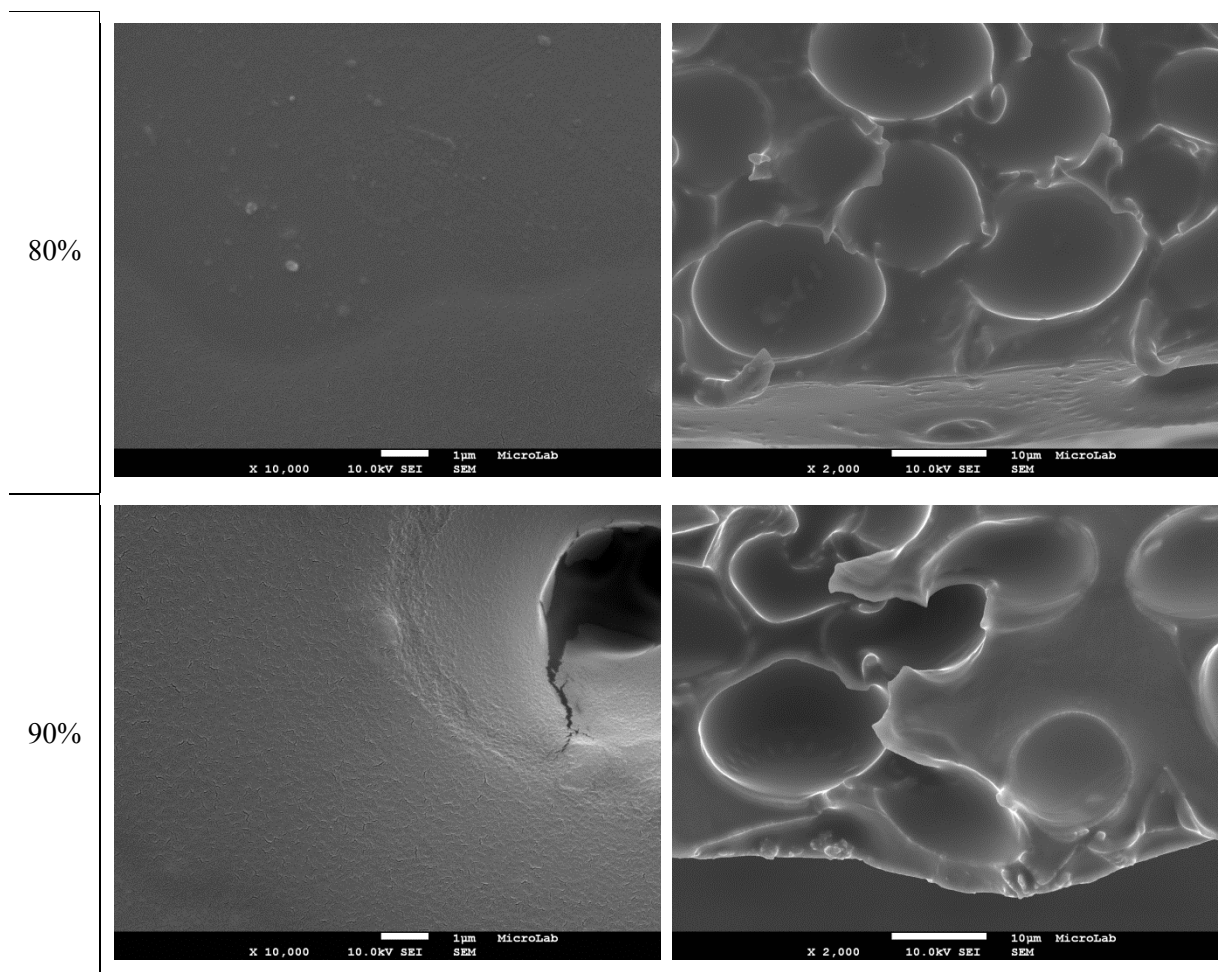
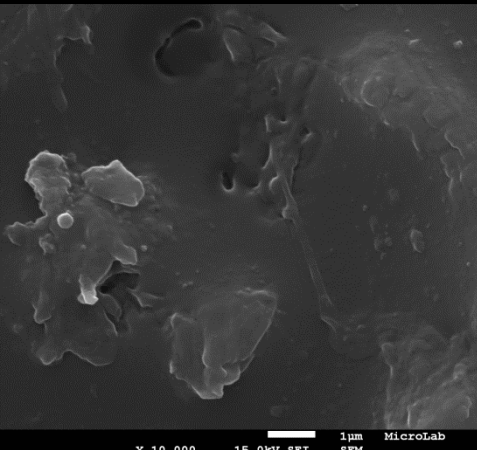
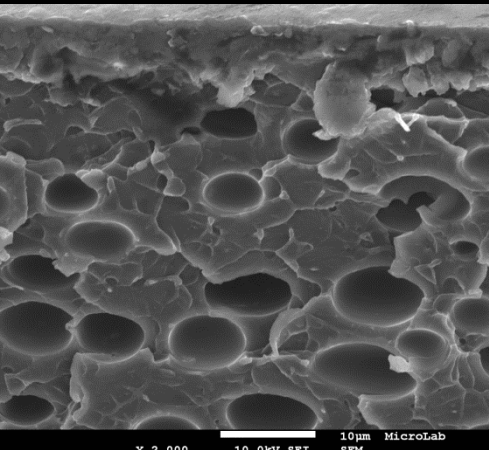
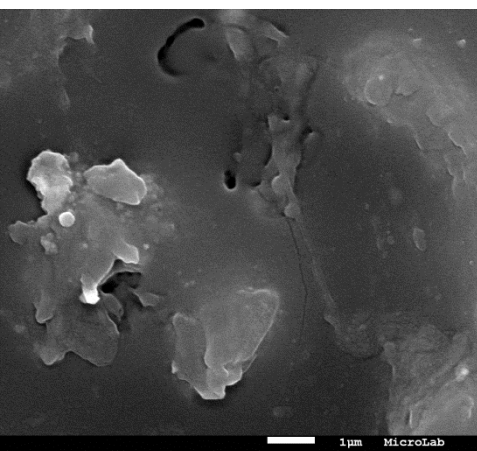
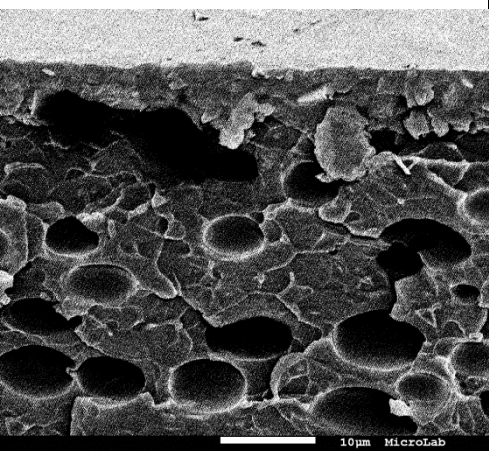
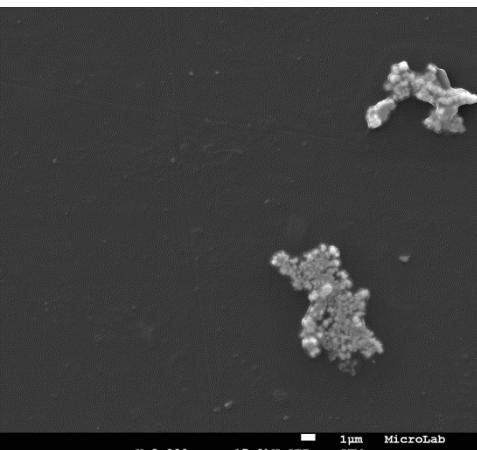
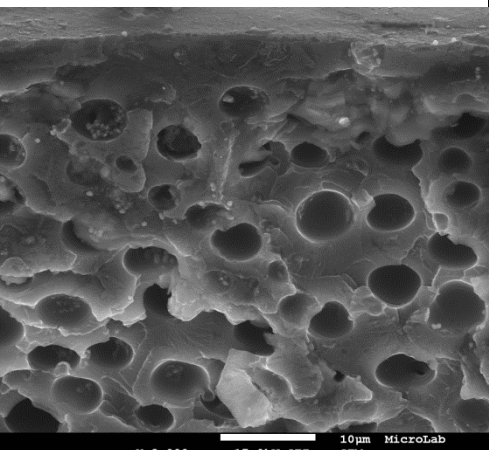


Figure 4. 2. Scanning Electron Microscopy images of the Matrimid membranes with different IL %

It is apparent from the above Figure 4.2., that though the surface remained smooth with increasing % IL the membrane porosity increased as can be seen in the cross sectional pictures. It appears that there is a thin dense film on the surface. The membrane with 20% IL has an increased number of surficial pores which can be due to accelerated drying of the membrane during synthesis. Most of the membranes were homogeneous and any observable surface distortions can be attributed to mild variations in conditions during polymerization and drying of the membrane.



DEVELOPMENT OF MIXED MATRIX MEMBRANES WITH METAL – ORGANIC FRAMEWORKS AND IONIC LIQUIDS FOR BIOGAS UPGRADING

MOF	SEM Mode	Surface	Cross-section
<b>Cu<sub>3</sub>(BTC)<sub>2</sub></b>	SE		
	BSE		
<b>MIL - 101</b>	SE		

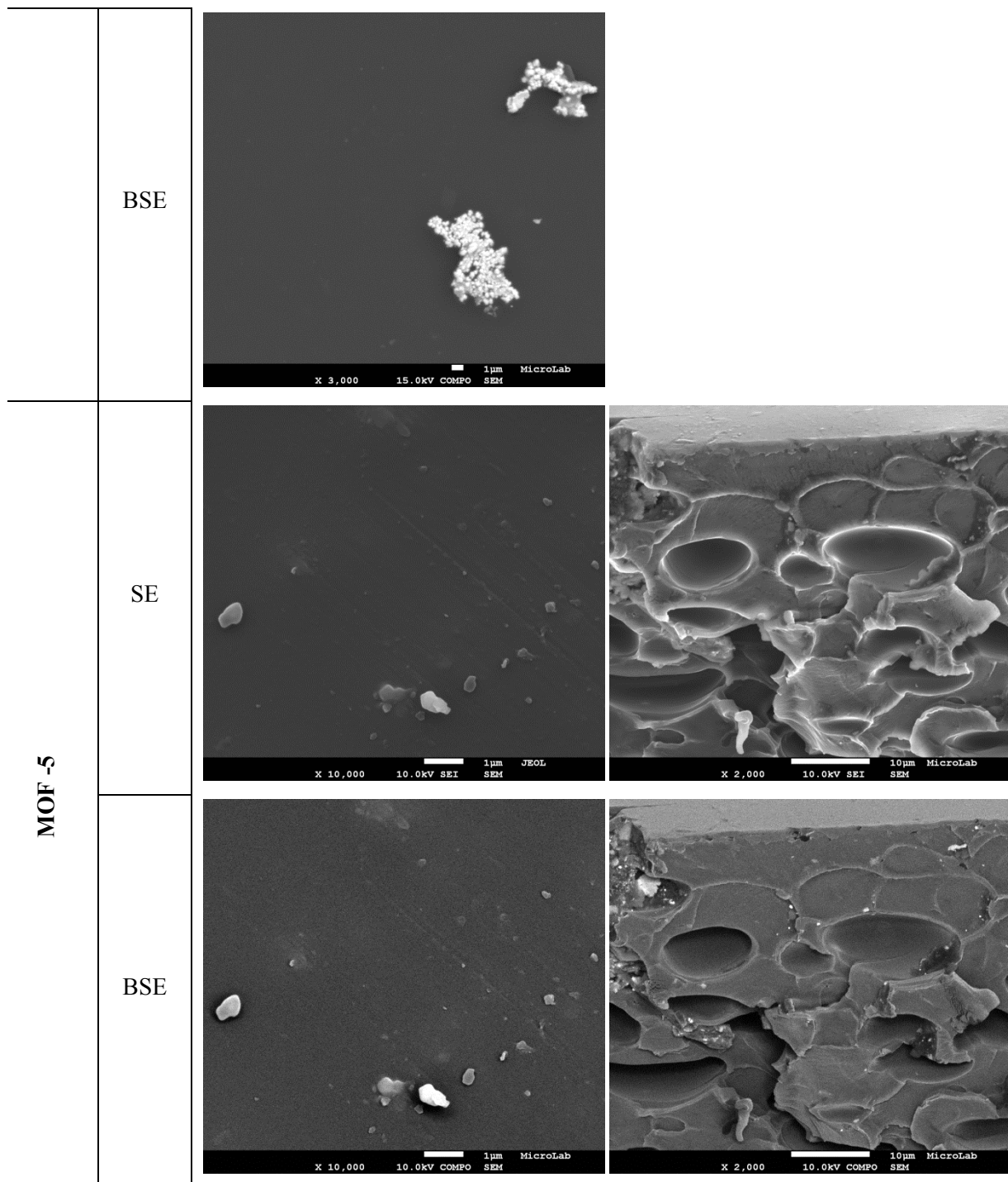


Figure 4. 3. SEM images of the Matrimid membranes with 50% IL and 20% MOFs -  $\text{Cu}_3(\text{BTC})_2$ , MIL101 and MOF-5 with Secondary electron emission (SE) and Back-scattered electron emission mode (BSE).

Figure 4.3 shows scanning electron microscopy images of the Matrimid membranes synthesized with 50% IL  $[\text{bmim}][\text{Tf}_2\text{N}]$  loading and 20% loading of three different MOFs –  $\text{Cu}_3(\text{BTC})_2$ , MIL101 and MOF-5. The samples were scanned in two modes – secondary electron (SE) emission and back-scattered electron (BSE) emission. The back-scattered electrons are electrons of the original electron beam (incident) reflected or scattered when they encounter the atomic nuclei of the surface being scanned. These electrons are useful in imaging the sample to greater depth and when



the sample contains higher atomic number (metals) components. Since our samples contained MOFs it was useful to image them using BSE mode as is apparent from the images in Figure 4.3., the MOFs are highlighted compared to rest of the surface i.e., the MOFs appear as very bright zones or spots. From the SEM images of the membrane cross-section in Figure 4.3., it can be seen that the membranes have maintained the same level of porosity as seen in the membranes with just Matrimid and 50% IL in Figure 4.2. However, the MOF particles do not seem to have distributed uniformly and can be seen to have formed aggregates in all the membranes. This is very clear in the BSE images of both the surface and cross section of the samples. In the case of the membrane with  $\text{Cu}_3(\text{BTC})_2$  the MOF aggregates seem to have caused defects and probably cracks on the membrane surface which may lead to unusual performance characteristics of this membrane.

#### 4.4. Mechanical Properties

Membrane gas separation processes are usually operated at high pressure to obtain optimum throughput hence it is crucial that the membrane be able to withstand the same. Testing the puncture resistance and durability of the membrane is an essential check before application of the membrane for gas separation.

##### 4.4.1. Puncture test

Usually upgrading plants are operated under high pressures to ensure high throughput of gas. Hence it is important that the membrane should be able to withstand higher stress than the operating pressures. The puncture test helps to determine the stress (expressed in terms of pressure) at which the membrane will breach. The stress strain data for the membranes produced in the present work can be seen in Table 4.4.1.

Table 4.4.1. Puncture test stress - strain data with membrane thickness for varied IL loading

% IL	Thickness (mm)	% Elongation at break	$\sigma_{\text{Elongation}}$	Stress at break [MPa]	$\sigma_{\text{Stress}}$
0%	0.064 ±0.0020	6.63	0.31	7.37	0.30
5%	0.060 ±0.0054	10.26	3.63	9.33	2.60
25%	0.046 ±0.0076	6.50	1.18	4.15	0.07
30%	0.073 ±0.0076	1.51	0.03	2.18	0.13
40%	0.074 ±0.0029	8.60	1.40	5.51	0.66
50%	0.412 ±0.0250	13.04	1.40	15.17	0.86
80%	0.394 ±0.0251	10.17	0.71	12.22	0.45
90%	0.284 ±0.0712	7.82	1.54	8.27	1.05

\* $\sigma_{\text{Elongation}}$ ,  $\sigma_{\text{Stress}}$  - Standard deviation for elongation at break and stress at break respectively

Although there are several discrepancies, it can be noted that addition of ionic liquid did not improve the membrane stress tolerance compared to the neat Matrimid membrane. But it can be seen that the membranes are able to tolerate much higher pressures (up to 70 bar) than operating conditions which are usually run at up to 10 bar [2].

**Table 4.4. 2. Puncture test stress - strain data with membrane thickness for membranes with MOFs and IL**

<b>% Loading</b>	<b>Thickness (mm)</b>	<b>% Elongation at break</b>	$\sigma_{\text{Elongation}}$	<b>Stress at break [MPa]</b>	$\sigma_{\text{Stress}}$
<b>50% IL + 20% Cu<sub>3</sub>(BTC)<sub>2</sub></b>	0.475 ±0.04	3.75	0.5	5.63	0.36
<b>50% IL + 20% MIL101</b>	0.400 ±0.06	2.76	0.96	4.95	1.17
<b>50% IL + 20% MOF5</b>	0.367 ±0.02	8.3	1.5	7.93	0.07

*\* $\sigma_{\text{Elongation}}$ ,  $\sigma_{\text{Stress}}$  - Standard deviation for elongation at break and stress at break respectively*

Stress strain data for membranes loaded with 20% MOF and 50% IL can be seen in Table 4.4.2. When conducting the test for these membranes a fracture profile with multiple peaks was observed further confirming that the MOF particles aggregate to form surface defects and weaken the membrane. The puncture stress and elongation at break are dependent on the membrane thickness. Hence the results obtained for 50%, 80% and 90% ionic liquid loaded membranes and 20% MOF with 50% IL loaded membranes cannot be directly compared to the other membranes as their thickness is significantly higher. There is very limited data available regarding the mechanical properties of Matrimid based membranes. Zhang et al [66] report that the stress at break and elongation at break are 87.1 MPa and 21.1% respectively for neat Matrimid membrane and decreases significantly with MOF loading due to aggregation of the MOF weakening the membrane. However they do not report the membrane thickness hence it is difficult to compare. Another report by Basu et al [4]., is about polyimide membranes wherein the membranes have an average thickness of 40-60  $\mu\text{m}$  and they show similar values of stress at break and elongation at break to Zhang et al., i.e., 105 MPa and 119% respectively. Based on these results it seems that the membranes prepared in the present study are either too thin or too porous but have sufficient mechanical stability for the desired purpose.

## 4.5. Gas Permeability

As mentioned earlier, biogas contains 60% methane and 40% CO<sub>2</sub>. In order to obtain clean burning fuel grade bio methane, the CO<sub>2</sub> has to be reduced to less than 2% (v/v) of the gas. The main purpose of this work is to develop a membrane which can effectively perform this task. Hence testing the permeability of CO<sub>2</sub> and CH<sub>4</sub> through prepared membranes is the most important experiment. The basis of gas separation using membranes is the difference in permeability of different gases with respect to the membrane. The solution - diffusion model is the most accepted mechanism of transport of solutes or components across the membrane with respect to dense membrane based gas separations. According to this model, a component's permeability across a given membrane is a function of its ability to "absorb" into the membrane and then "diffuse" across it to the permeate side. In the present experiment the permeability of individual gases was determined using the method described by Cussler et al [65] at a temperature of 30°C. The table 4.5.1 below shows the permeability and selectivity values obtained for different membrane composition when testing individually with CO<sub>2</sub> and methane.

**Table 4.5. 1. Membrane Permeation data**

Membrane Composition	Permeability [m <sup>2</sup> /s]		Permeability [Barrer*]				Selectivity αCO <sub>2</sub> /CH <sub>4</sub>
	CH <sub>4</sub>	CO <sub>2</sub>	CH <sub>4</sub>	σ <sub>CH<sub>4</sub></sub>	CO <sub>2</sub>	σ <sub>CO<sub>2</sub></sub>	
<b>Matrimid</b>	5x10 <sup>-13</sup>	1x10 <sup>-11</sup>	0.60	0.03	12.05	0.04	20.00
<b>Matrimid +5% IL</b>	7x10 <sup>-13</sup>	1x10 <sup>-11</sup>	0.84	0.31	12.05	0.07	14.29
<b>Matrimid +25% IL</b>	1x10 <sup>-12</sup>	7x10 <sup>-12</sup>	1.20	0.28	8.43	0.07	7.00
<b>Matrimid +30% IL</b>	6x10 <sup>-13</sup>	8x10 <sup>-12</sup>	0.72	0.42	9.64	0.71	13.33
<b>Matrimid +40% IL</b>	2x10 <sup>-12</sup>	1x10 <sup>-11</sup>	2.41	0.85	12.05	0.04	5.00
<b>Matrimid +50% IL</b>	2x10 <sup>-12</sup>	2x10 <sup>-11</sup>	2.41	0.87	24.10	0.46	10.00
<b>Matrimid +80% IL</b>	4x10 <sup>-12</sup>	3x10 <sup>-11</sup>	4.82	1.85	36.14	0.30	7.50
<b>Matrimid +90% IL</b>	3x10 <sup>-12</sup>	2x10 <sup>-11</sup>	3.61	1.91	24.10	1.75	6.67
<b>Matrimid+50%IL+20%MOF 5</b>	4x10 <sup>-12</sup>	2x10 <sup>-11</sup>	4.82	0.79	24.10	0.34	5.00
<b>Matrimid+50%IL+20%MIL 101</b>	1x10 <sup>-11</sup>	3x10 <sup>-11</sup>	12.05	0.75	36.14	2.07	3.00
<b>Matrimid+50%IL+20%Cu<sub>3</sub>(BTC)<sub>2</sub></b>	7x10 <sup>-10</sup>	2x10 <sup>-10</sup>	843.37	21.93	240.96	1.64	0.29

\*1 Barrer = 7.5005 x 10<sup>-18</sup> m<sup>2</sup>·s<sup>-1</sup>·Pa<sup>-1</sup>

\*\*σ - Standard deviation

From the data in the table above and the curve shown in the Figure 4.5.1., it is apparent that as the IL concentration increases, so does the CO<sub>2</sub> and CH<sub>4</sub> permeability. But it is also clear that the membrane is more selectively permeable to CO<sub>2</sub> and hence these membranes could be considered for further testing for biogas upgrading.

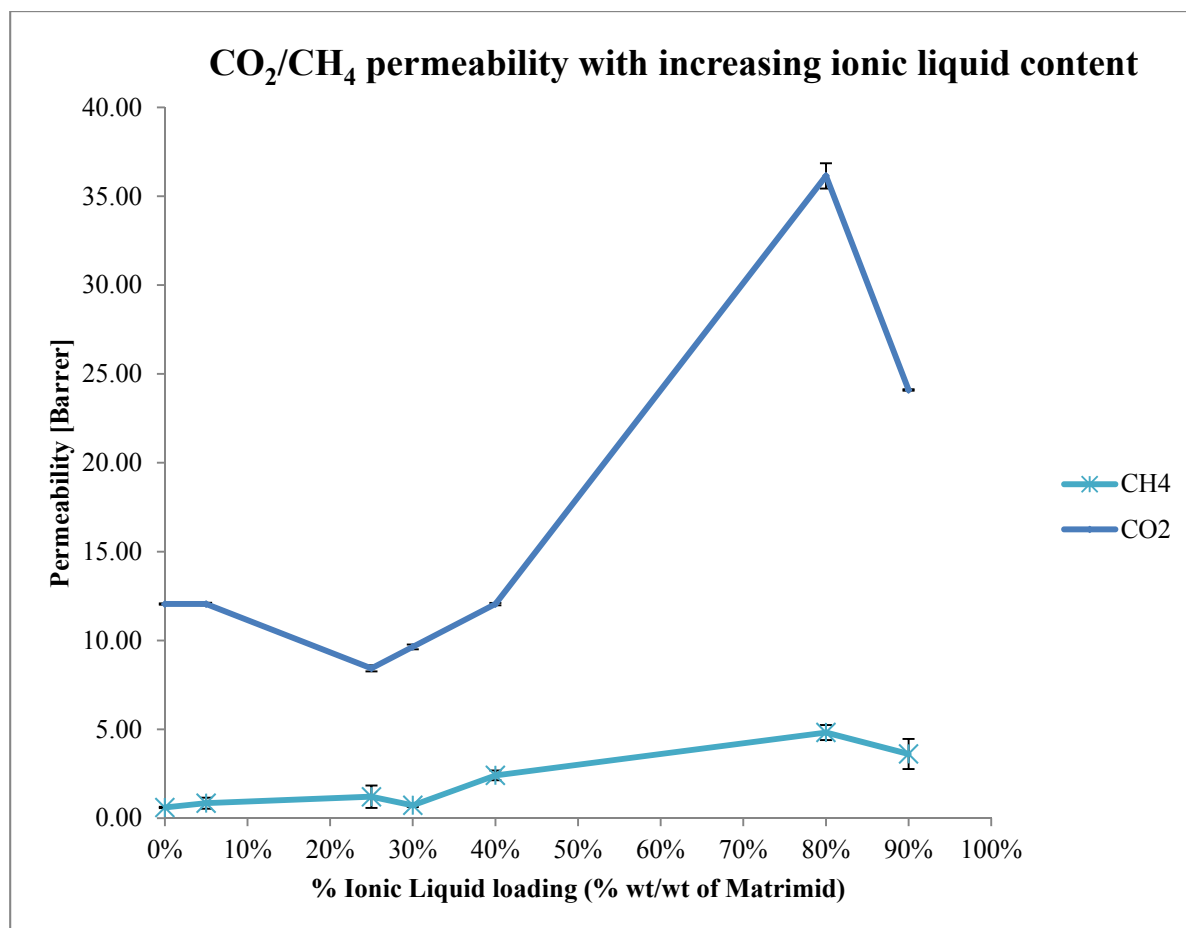


Figure 4.5. 1. CO<sub>2</sub>/ CH<sub>4</sub> Permeability with increasing Ionic liquid content

Neglecting the errors, these permeability results follow a trend similar to that observed by Kanehashi et . al., [11] where in the same ionic liquid ([bmim][Tf<sub>2</sub>N]) was used but with a different polyimide material and membranes were formed and tested under similar conditions. They have noted that it was not possible to load IL into the membrane beyond 80% as it tended not to imbue into the matrix. Similar problem was observed in the present work when attempts were made to synthesize membranes loaded with 80% IL and 20% MOF, wherein the membrane formed defectively, hence it was decided to use a lower IL loading for further study.

Figure 4. 5. 2., shows the CO<sub>2</sub>/CH<sub>4</sub> separation performance of each Matrimid membranes at 30°C with other similar membranes for comparison and the empirical upper bound cited in literature by Robeson [67]. As can be observed the performance of the membranes produced in this work is considerably lower than the empirical upperbound defined both in terms of permeability and selectivity. In comparison to similar works by Basu et al., [4] and Meek et al.,[53] the membranes in the present work have much higher permeability for CO<sub>2</sub> but have lower selectivity. In fact the permeability and selectivity of Matrimid without additives is higher than the membranes with additives.

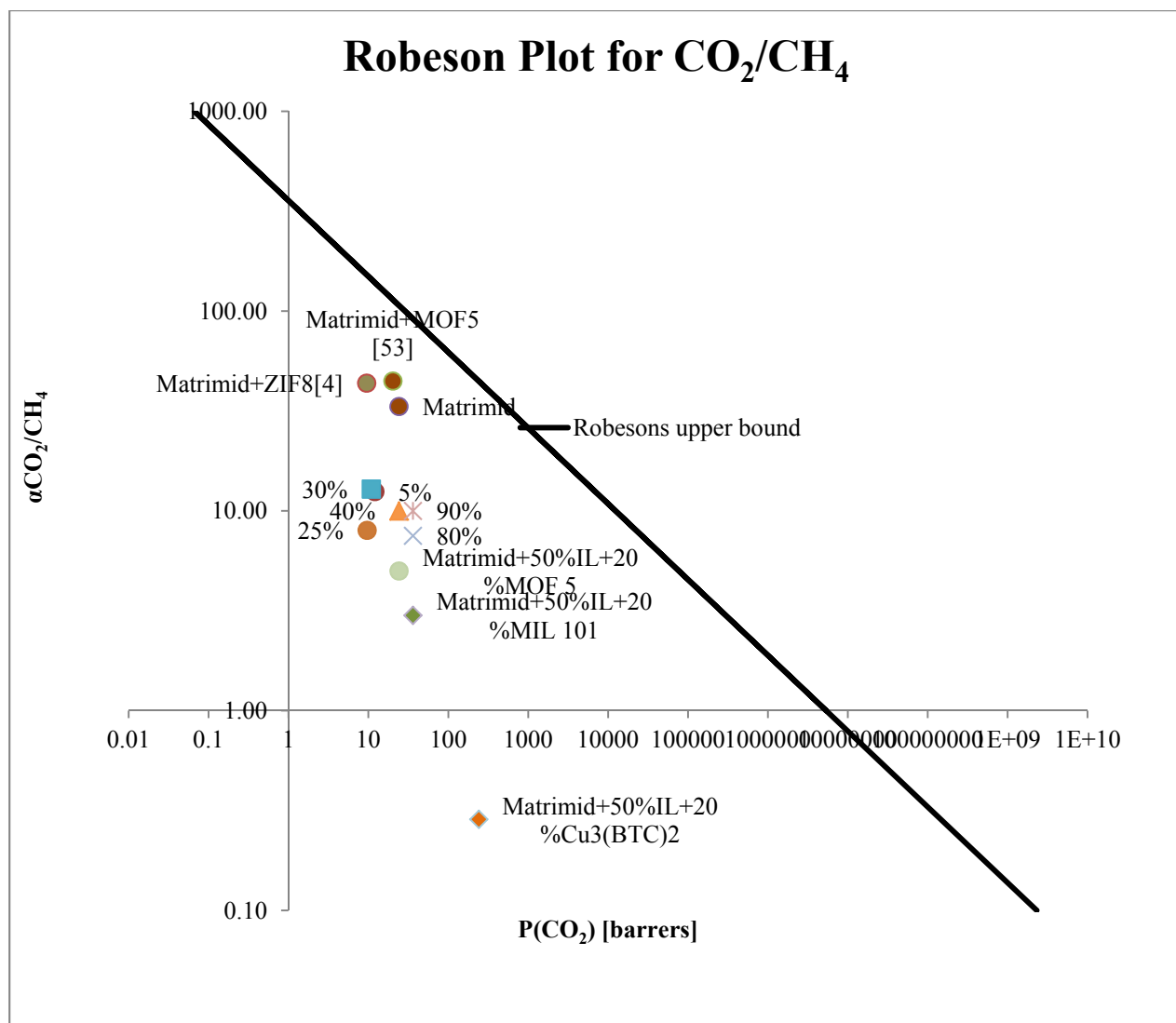


Figure 4.5. 2. Complete Robeson plot for CO<sub>2</sub>/CH<sub>4</sub> with results from the current work

As can be seen in Figure 4.5.2., it was found that the membrane with 20% Cu<sub>3</sub>(BTC)<sub>2</sub> and 50% IL had the highest CO<sub>2</sub> and CH<sub>4</sub> permeability of 240 barrer and 843 barrer respectively but the membrane was more selective for CH<sub>4</sub> than for CO<sub>2</sub> (α<sub>CO<sub>2</sub>/CH<sub>4</sub> = 0.28) this was in strong contrast with that reported in literature by Basu et al.[4] who claim to have achieved α<sub>CO<sub>2</sub>/CH<sub>4</sub> = 30 using the same MOF with polyimide membrane without IL loading. It could be attributable to the membrane aberrations caused by the MOF aggregates as seen in the SEM images of the membrane.</sub></sub>

The membrane with 20% MOF 5 and 50% IL had a CO<sub>2</sub> and CH<sub>4</sub> permeability of 24 barrer and 4.82 barrer respectively and membrane with 20% MIL 101 and 50% IL had CO<sub>2</sub> and CH<sub>4</sub> permeability of 36.14 barrer and 12.05 barrer respectively as compared to the neat Matrimid membrane which had CO<sub>2</sub> and CH<sub>4</sub> permeability of 12.05 barrer and 0.6 barrer respectively. Overall

the mixed matrix membranes loaded with both MOF and IL showed low selectivity but better permeability than neat Matrimid membrane. At the time of this work there were no reports in literature of mixed matrix Matrimid membranes prepared with both MOFs and ILs hence direct comparison was not possible.

---

## 5. CONCLUSIONS AND FUTURE WORK

---

In the present work efforts were made to develop mixed matrix membranes with both ionic liquid and MOF dispersed in the matrix for the purpose of biogas upgrading. Initial studies revealed that chloroform is not a suitable solvent for synthesis of Matrimid mixed matrix membrane with ionic liquid [bmim][Tf<sub>2</sub>N] and since stable membranes were obtained with dichloromethane studies were continued with the same.

Matrimid membranes with different loading of ionic liquid (from 5% to 90%) were synthesized and it was found that the CO<sub>2</sub> permeability of the membrane increases with increase in IL loading. It was also found that the hydrophilicity improved with increase in IL loading but the puncture resistance did not improve. Based on these results it was decided to synthesize Matrimid mixed matrix membranes with 20% MOF loading and 80% IL loading but the membranes formed were defective. Hence, it was decided to synthesize membranes with 50% IL and 20% MOF loading. Stable membranes were obtained and were used for further studies.

Three different MOFs were used – MIL101, Cu<sub>3</sub>(BTC)<sub>2</sub> and MOF-5 at loading of 20% and their performances were tested for hydrophilicity and gas permeability. It was found that the membrane with 20% MOF 5 and 50% IL had the smallest contact angle of 59°53' while the membrane with 20% Cu<sub>3</sub>(BTC)<sub>2</sub> and 50% IL had a contact angle of 75° and membrane with 20% MIL 101 and 50% IL had a contact angle of 81°27' as compared to the neat Matrimid membrane which had a contact angle of 81°. From the scanning electron microscopy images of these membranes it was observed that the MOFs tend to aggregate and cause surface aberrations – this was very apparent in the membrane with the MOF Cu<sub>3</sub>(BTC)<sub>2</sub> and it reflected in its gas permeation performance. In the puncture tests the membranes with MOF were found to have a fracture profile due to membrane weakening by MOF aggregates.

Based on the gas permeation experiments it was found that the membrane with 20% Cu<sub>3</sub>(BTC)<sub>2</sub> and 50% IL had the highest CO<sub>2</sub> and CH<sub>4</sub> permeability of 240 barrer and 843 barrer respectively but the membrane was more selective for CH<sub>4</sub> than for CO<sub>2</sub> ( $\alpha_{\text{CO}_2/\text{CH}_4}$ ) this was in strong contrast with that reported in literature. The membrane with 20% MOF 5 and 50% IL had a CO<sub>2</sub> and CH<sub>4</sub> permeability of 24 barrer and 4.82 barrer respectively and membrane with 20% MIL 101 and 50% IL had CO<sub>2</sub> and CH<sub>4</sub> permeability of 36.14 barrer and 12.05 barrer respectively as compared to the neat Matrimid membrane which had CO<sub>2</sub> and CH<sub>4</sub> permeability of 12.05 barrer and 0.6 barrer respectively. Overall the mixed matrix membranes loaded with both MOF and IL showed low selectivity but better permeability than neat Matrimid membrane. At the time of this work there were no reports in literature of mixed matrix Matrimid membranes prepared with both MOFs and ILs hence direct comparison was not possible.



Further analysis like thermogravimetry, FTIR spectroscopy and X-ray diffraction studies are necessary to determine the actual MOF and IL loading in the formed membrane to understand the mechanism of gas transfer but due to the time limitations these tests could not be performed.

Preparing membranes with other MOFs and task specific ILs at different loadings simultaneously with different IL loading would be an interesting study. Also changing the base polymer to other popular ones like 6FDA based polyimide and PVAc could be tried to improve selectivity of membrane.

---

## 6. REFERENCES

---

1. AEBIOM. 2012: European Biomass Association. A Biogas Road Map for Europe. Available <http://www.aebiom.org/?p=231#more-231>. Accessed 3rd June 2013.
2. Zhang, Y., Sunarsoc, J., Liud, S., and R. Wang. Current status and development of membranes for CO<sub>2</sub>/CH<sub>4</sub> separation: A review. *International Journal of Greenhouse Gas Control* 12 (2013) 84–107.
3. Houde, A. Y., B. Krishnakumar, S. G. Charati and S. A. Stern, Permeability of dense (homogeneous) cellulose acetate membranes to methane, carbon dioxide, and their mixtures at elevated pressures, *J. Appl. Polym. Sci.*, 1996, 62, 2181- 2192.
4. Basu, S., Cano-Odena, A., and I. Vankelecom. MOF-containing mixed-matrix membranes for CO<sub>2</sub>/CH<sub>4</sub> and CO<sub>2</sub>/N<sub>2</sub> binary gas mixture separations. *Separation and Purification Technology* 81 (2011) 31–40.
5. Car, A., Stropnik, C., and K. Peinemann. Hybrid membrane materials with different metal–organic frameworks (MOFs) for gas separation. *Desalination* 200 (2006) 424–426.
6. Anthony, J. L. (2004). Ph.D. Thesis, Gas Solubilities in Ionic Liquids: Experimental Measurements and Applications. University of Notre Dame, Indiana.
7. Cadena, C.; Anthony, J. L.; Shah, J. K.; Morrow, T. I.; Brennecke, J. F. Maginn E. J. (2004). Why is CO<sub>2</sub> so soluble in Imidazolium-based Ionic Liquids? *J. American Chem. Society.*, 126, 5300-5308.
8. Bates, E. D.; Mayton, R. D.; Ntai, I.; Davis, J. H. (2002). CO<sub>2</sub> Capture by a Task-Specific Ionic Liquid., *J. Amer. Chem. Soc.*, Vol. 124, No. 6, 926-927.
9. Neves, L. A., Afonso, C., Coelho, I. M., and J.G. Crespo. Integrated CO<sub>2</sub> capture and enzymatic bioconversion in supported ionic liquid membranes. *Separation and Purification Technology* 97 (2012) 34–41
10. Neves, L. A., Coelho, I. M., and J.G. Crespo. Gas permeation studies in supported ionic liquid membranes. *Journal of Membrane Science* 357 (2010) 160–170.
11. Kanehashi, S., Kishida, M., Kidesaki, T., Shindo, R., Sato, S., Miyakoshi, T., and K. Nagai. CO<sub>2</sub> separation properties of a glassy aromatic polyimide composite membranes containing high-content 1-butyl-3-methylimidazolium bis(trifluoromethylsulfonyl)imide ionic liquid. *Journal of Membrane Science* 430 (2013) 211–222.
12. EU Commission. 2006. Communication from the commission. An EU Strategy for Biofuels. Available: <http://eurlex.europa.eu/LexUriServ/LexUriServ.do.uri=COM:2006:0034:FIN:EN:PDF>. Accessed 15.05.2013.
13. Rasi, S. 2009. Biogas Composition and Upgrading to Biomethane. University of Jyväskylä. Ph.D. Dissertation

14. Persson, M. 2003: Evaluation of Upgrading Techniques for Biogas. Available [www.sgc.se/dokument/Evaluation.pdf](http://www.sgc.se/dokument/Evaluation.pdf). Accessed 03.05.2013.
15. Ryckebosch, E. Drouillon, M., Vervaeren, H. 2011: Techniques for Transformation of Biogas to Biomethane. *Journal of Biomass and Bioenergy* 35 1633-1645.
16. Urban, W., Girod, K., Lohmann, H., 2009: Technologien und Kosten der Biogasaufbereitung und Einspeisung in das Erdgasnetz. Ergebnisse der Markterhebung 2007–2008. 123 s. Fraunhofer-Institut für Umwelt-, Sicherheits- und Energietechnik, Oberhausen (German).
17. Alterner Programme. 2001: Adding biomass to the gas grid. Available [www.dgc.eu/pdf/altener.pdf](http://www.dgc.eu/pdf/altener.pdf) . Accessed 03.05.2013.
18. Baker, R. W., Future directions of membrane gas separation technology, *Ind. Eng. Chem. Res.*, 2002, 41, 1393-1411.
19. te Hennepe, H.J.C., et al., Zeolite-filled silicone rubber membranes Experimental determination of concentration profiles. *Journal of Membrane Science*, 1994.89(1-2): p. 185.
20. Duval, J.M., et al., Adsorbent filled membranes for gas separation. Part 1. Improvement of the gas separation properties of polymeric membranes by incorporation of microporous adsorbents. *Journal of Membrane Science*, 1993. 80(1): p. 189.
21. Duval, J.M., et al., Preparation of zeolite filled glassy polymer membranes. *Journal of Applied Polymer Science*, 1994. 54(4): p. 409.
22. Li, Y., et al., The effects of polymer chain rigidification, zeolite pore size and pore blockage on polyethersulfone (PES)-zeolite A mixed matrix membranes. *Journal of Membrane Science*, 2005. 260(1-2): p. 45.
23. Suer, M.G., N. Bac, and L. Yilmaz, Gas permeation characteristics of polymer-zeolite mixed matrix membranes. *Journal of Membrane Science*, 1994. 91(1-2).
24. Kim, S., T.W. Pechar, and E. Marand, Poly(imide siloxane) and carbon nanotube mixed matrix membranes for gas separation. *Desalination*, 2006. 192(1-3): p. 330.
25. Vu, D.Q., W.J. Koros, and S.J. Miller, Mixed matrix membranes using carbon molecular sieves: I. Preparation and experimental results. *Journal of Membrane Science*, 2003. 211(2): p. 311.
26. Paul, D., Y. Yampol'skii, *Polymeric gas separation membranes*, Baton rouge: CRC Press, 1994.
27. Rousseau, R.W., *Handbook of separation process technology*, John Wiley & Sons, New York, 1987.
28. Stannett, V., W. Koros, D. Paul, H. Lonsdale, R. Baker, Recent advances in membrane science and technology, in: *Chemistry*, 1979, pp. 69-121.
29. Brydson, J. A, *Plastics materials*, Butterworth-Heinemann, 1999.

30. Ohya, H., V.V. Kudryavsev, S.I. Semenova, *Polyimide Membranes: Applications, Fabrications and Properties*, CRC Press, 1997.
31. Chung, T., W. H. Lin, R.H. Vora, Gas transport properties of 6FDA-durene/1,3-phenylenediamine (mPDA) copolyimides, *J. Appl. Polym. Sci.*, 81 (2001) 3552-3564.
32. Ohya, H., V.V. Kudryavsev, S.I. Semenova, Chapter 6, in: *Polyimide Membranes: Applications, Fabrications and Properties*, CRC Press, 1997.
33. Bos, A., I.G.M. Punt, M. Wessling, H. Strathmann, Plasticization-resistant glassy polyimide membranes for CO<sub>2</sub>/CH<sub>4</sub> separations, *Separation and Purification Technology*, 14 (1998) 27-39.
34. Clausi, D. T., W.J. Koros, Formation of defect-free polyimide hollow fiber membranes for gas separations, *J. Membr. Sci.*, 167 (2000) 79-89.
35. Rogers, R. D.; Seddon, K. R.; Volkov, S. (2000). *Green industrial applications of ionic liquids*. Kluwer Academic Publishers, The Netherlands.
36. Brennecke, J. F.; Maginn, E. J. (2001). Ionic liquids: innovative fluids for chemical processing. *AIChE J.*, 47, 2384-2389.
37. Anthony, J. L.; Maginn E. J.; Brennecke, J. F. (2002). Solubilities and Thermodynamic Properties of Gases in the Ionic Liquid 1-n-Butyl-3-methylimidazolium Hexafluorophosphate. *J. Phys. Chem. B*, 106, 7315-7320.
38. Kazarian, S. G.; Briscoe, B. J.; Welton, T. (2000). Combining ionic liquids and supercritical fluids: in situ ATR-IR study of CO<sub>2</sub> dissolved in two ionic liquids at high pressures. *Chem. Commun.*, 20, 2047-2048.
39. Anthony, J. L.; Anderson, J. L.; Maginn E. J.; Brennecke, J. F. (2005). Anion Effects on Gas Solubility in Ionic Liquids. *J. Phys. Chem. B*, 109, 6366-6374.
40. Lee, B. C.; Outcalt, S. L. (2006). Solubilities of Gases in the Ionic Liquid 1-n- Butyl-3-methylimidazolium Bis(trifluoromethylsulfonyl)imide. *J. Chem. Eng. Data*, 51, 892-897.
41. Seader, J. D.; Henley, E. J. (1998). *Separation Process Principles*. 1st edition, John Wiley & Sons Inc., New York.
42. Mulder, M. (2003). *Basic Principles of Membrane Technology*, 2nd edition. Kulwer Academic Publishers, The Netherlands.
43. Hao, L., Li, P., Yang, T., and T. Chung. Room temperature ionicliquid/ZIF-8 mixed-matrix membranes for natural gas sweetening and post-combustion CO<sub>2</sub> capture. *Journal of Membrane Science* 436(2013)221–231.
44. Bao, Z., Alnemrat, s., Yu, L., Vasiliev,I., Ren, Q., Lu, X., and S. Deng. Kinetic separation of carbon dioxide and methane on a copper metal–organic framework. *Journal of Colloid and Interface Science* 357 (2011) 504–509.

45. Josephine, M., Ordoñez, C., Balkus, K. J., Ferraris, J. P., and I. H. Musselman. Molecular sieving realized with ZIF-8/Matrimid® mixed-matrix membranes. *Journal of Membrane Science* 361 (2010) 28–37.
46. Yang, T., and T Chung. High performance ZIF-8/PBI nano-composite membranes for high temperature hydrogen separation consisting of carbon monoxide and water vapour. *Int. J. Hyd Energy* 38 (2013) 229 - 239.
47. Finsy, V., Maa, L., Alaerts, L., De Vos, D. E., Baron, G. V., and J.F.M. Denayer. Separation of CO<sub>2</sub>/CH<sub>4</sub> mixtures with the MIL-53(Al) metal–organic framework. *Microporous and Mesoporous Materials* 120 (2009) 221–227.
48. Liu, Y., Hu, E., Khan, E. A., and Z. Lai. Synthesis and characterization of ZIF-69 membranes and separation for CO<sub>2</sub>/CO mixture. *Journal of Membrane Science* 353 (2010) 36–40.
49. Liu, Y., Zeng, G., Pan, Y., and Z. Lai. Synthesis of highly c-oriented ZIF-69 membranes by secondary growth and their gas permeation properties. *Journal of Membrane Science* 379 (2011) 46– 51.
50. Li, Y., Liang, F., Bux, H., Yang, W., and J. Caro. Zeolitic imidazolate framework ZIF-7 based molecular sieve membrane for hydrogen separation. *Journal of Membrane Science* 354 (2010) 48–54.
51. Li, T., Pan, Y., Peinemann, K., and Z. Lai. Carbon dioxide selective mixed matrix composite membrane containing ZIF-7 nano-fillers. *Journal of Membrane Science* 425-426 (2013) 235–242.
52. Adams, R., Carson, C., Ward, J., Tannenbaum, R. and W. Koros. Metal organic framework mixed matrix membranes for gas separations. *Microporous and Mesoporous Materials* 131 (2010) 13–20.
53. Meek, S. T., Greathouse, J. A., and M. D. Allendorf. Metal-Organic Frameworks: A Rapidly Growing Class of Versatile Nanoporous Materials *Adv. Mater.* 2011, 23, 249–267.
54. Yoo, Y., Lai, Z., and H. Jeong. Fabrication of MOF-5 membranes using microwave-induced rapid seeding and solvo-thermal secondary growth. *Microporous and Mesoporous Materials* 123 (2009) 100–106
55. Perez, E. V., Balkus, K. J., Ferraris, J. P., and Inga H. Musselman. Mixed-matrix membranes containing MOF-5 for gas separations. *Journal of Membrane Science* 328 (2009) 165–173.
56. Cejka J. *Metal-Organic Frameworks Applications from Catalysis to Gas Storage.* Weinheim, Wiley-VCH, 2011.

57. Bae, T., Lee, J. S., Qiu, W., Koros, W. J., Jones, C. W., and S. Nair. A High-Performance Gas-Separation Membrane Containing Submicrometer-Sized Metal–Organic Framework Crystals. *Angew. Chem. Int. Ed.* 2010, 49, 9863 –9866.
58. Zou, X., Zhang, F., Thomas, S., Zhu, G., Valtchev, V., and S. Mintova.  $\text{Co}_3(\text{HCOO})_6$  Microporous Metal–Organic Framework Membrane for Separation of  $\text{CO}_2/\text{CH}_4$  Mixtures. *Chem. Eur. J.* 2011, 17, 12076 – 12083.
59. Zornoza, B., Martinez-Joaristi, A., Serra-Crespo, P., Tellez, C., Coronas, J., Gascon, J., and F. Kapteijn. Functionalized flexible MOFs as fillers in mixed matrix membranes for highly selective separation of  $\text{CO}_2$  from  $\text{CH}_4$  at elevated pressures. *Chem. Commun.*, 2011, 47, 9522–9524.
60. Chen, X. Y., Vinh-Thang, H., Rodrigue, D., and S. Kaliaguine. Amine-Functionalized MIL-53 Metal-Organic Framework in Polyimide Mixed Matrix Membranes for  $\text{CO}_2/\text{CH}_4$  Separation. *Ind. Eng. Chem. Res.* 2012, 51, 6895-6906.
61. Gupta, K. M., Chen, Y., Hu Z., and J. Jiang. Metal–organic framework supported ionic liquid membranes for  $\text{CO}_2$  capture: anion effects. *Phys. Chem. Chem. Phys.*, 2012, 14, 5785–5794
62. de Hullu, J., Maassen J.L.W., van Meel, P.A., Shazad, S., Vaessen J.M.P. 2008: Comparing Different Biogas Upgrading Techniques. Eindhoven University of Technology. Available <http://students.chem.tue.nl/ifp24/BiogasPublic.pdf> . Accessed 03.03.2012
63. Lems, R. & Dirkse, E.H.M. 2010: Small scale biogas upgrading: Green gas with the DMT Carborex-MS® system. 15th European Biosolids and Organic Resources Conference, organised by Aqua Enviro Technology Transfer. Available: [http://www.dirkse milieutechniek.com/dmt/do/download/\\_/true/210371/DMT\\_Carborex\\_MS\\_Small\\_scale\\_biogas\\_upgrading\\_Green\\_gas\\_1-11-2010.pdf](http://www.dirkse milieutechniek.com/dmt/do/download/_/true/210371/DMT_Carborex_MS_Small_scale_biogas_upgrading_Green_gas_1-11-2010.pdf). Accessed 15.4.2013.
64. Yuan, Y., and T. R. Lee. *Surface Science Techniques*. (Eds.) G. Bracco, B. Holst. 2013. ISBN: 978-3-642-34242-4
65. E.L. Cussler, *Diffusion*, second ed., Cambridge University Press, Cambridge, 1997.
66. Zhang, Y., Musselman, I. H., Ferraris, J. P., and K J. Balkus. Gas permeability properties of Matrimid® membranes containing the metal-organic framework Cu–BPY–HFS. *Journal of Membrane Science* 313 (2008) 170–181.
67. L. M. Robeson. The upper bound revisited. *Journal of Membrane Science* 320 (2008) 390–400.
68. Ahonen S. 2010. Alueellinen liikennebiokaasun tuotanto, siirto ja jakeluesimerkkitaipauksena Keski-Suomen maakunta (Finnish). University of Jyväskylä, Finland. Master’s thesis.

69. Avramescu, M.E., et al., Preparation of mixed matrix adsorber membranes for protein recovery. *Journal of Membrane Science*, 2003. 218(1-2): p. 219.
70. Ballinas, L., et al., Factors influencing activated carbon-polymeric composite membrane structure and performance. *Journal of Physics and Chemistry of Solids*, 2004. 65(2-3): p. 633.
71. Baxter-International, Composite membranes and methods to make such membranes. 1999, Patent WO0002638. p. 58.
72. Bhide, B. D. and S. A. Stern, Membrane processes for the removal of acid gases from natural gas. II. effects of operating conditions, economic parameters and membrane properties, *J. Membr. Sci.*, 1993, 81, 239-252.
73. Guan, H.-M., et al., Poly(vinyl alcohol) multilayer mixed matrix membranes for the dehydration of ethanol-water mixture. *Journal of Membrane Science*, 2006. 268(2): p. 113.
74. te Hennepe, H.J.C., et al., Zeolite-filled silicone rubber membranes : Part 1. Membrane preparation and pervaporation results. *Journal of Membrane Science*, 1987. 35(1): p. 39.
75. Lensmeyer, G.L., et al., Use of particle-loaded membranes to extract steroids for high-performance liquid chromatographic analyses improved analyte stability and detection. *Journal of Chromatography A*, 1995. 691(1-2): p. 239.
76. Lingeman, H. and S.J.F. Hoekstra-Oussoren, Particle-loaded membranes for sample concentration and/or clean-up in bioanalysis. *Journal of Chromatography B: Biomedical Sciences and Applications*, 1997. 689(1): p. 221.
77. Liu, Y., Ng, Z., Khan, E. A, Jeong, H., Ching, C., and Z. Lai. Synthesis of continuous MOF-5 membranes on porous  $\alpha$ -alumina substrates. *Microporous and Mesoporous Materials* 118 (2009) 296–301.
78. Llewellyn, P. L., Bourrelly, S., Serre, C., Vimont, A., Daturi, M., Hamon, L., Weireld, G., Chang, J., Hong, D., Hwang, Y. K., Jung, S. H., and G Fe'rey. High uptakes of  $\text{CO}_2$  and  $\text{CH}_4$  in Mesoporous Metal Organic Frameworks MIL-100 and MIL-101. *Langmuir* 2008, 24, 7245-7250.
79. Millipore, Cast membrane structures for sample preparation. 2000, Patent US6048457.
80. Pechar, T.W., et al., Preparation and characterization of a glassy fluorinated polyimide zeolite-mixed matrix membrane. *Desalination*, 2002. 146(1-3): p. 3.
81. Ratcliffe, C. T., A. Diaz, C. Nopasit, and G. Munoz, Application of membranes in  $\text{CO}_2$  separation from natural gas: pilot plant tests on offshore platforms, presented at the Laurence Reid Gas Conditioning Conference, Norman, OK, Feb. 21-24, 1999.
82. Tokuyama-Soda-Kabushiki-Kaisha, Microporous shaped article and process for preparation thereof. 1993, Patent US5238735.



---

## 7. APPENDICES

---

## Appendix I: Estimation of $\beta$

To find the geometric parameter “ $\beta$ ”, a PDMS membrane was used due to its well – known permeability. The test gas used was nitrogen. The feed and permeate pressure data obtained over time are represented in the Figure 7.1., below:

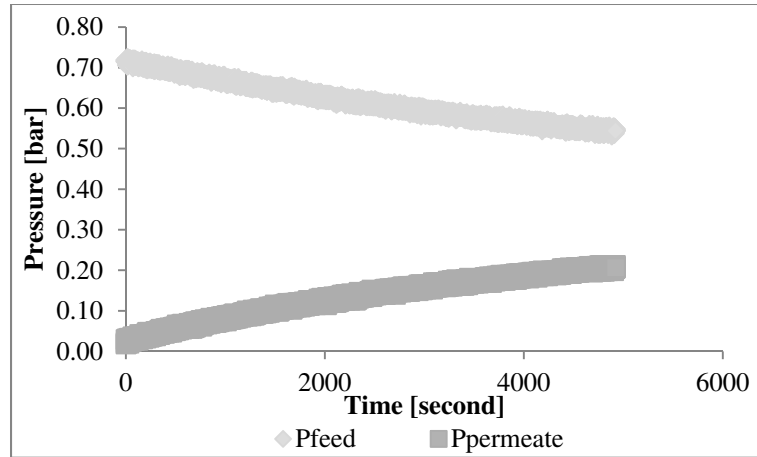


Figure 7. 1. Feed and Permeate Pressure Profiles in the permeation cell

By modifying equation 3.5.1., we can linearize it to the form shown below (Eq 7.1) and using nitrogen permeability value for the PDMS membrane referred to in bibliography the curve of  $\ln \frac{1}{P_i} \ln \left( \frac{\Delta p_0}{\Delta p} \right)$  versus  $\frac{t}{\delta}$  were traced, the slope of which gives the value of  $\beta$  ( $\beta = 48.079$ ) as shown in Figure 7.2.

$$\ln \frac{1}{P_i} \ln \left( \frac{\Delta p_0}{\Delta p} \right) = \beta \frac{t}{\delta} \dots \dots (Eq 7.1)$$

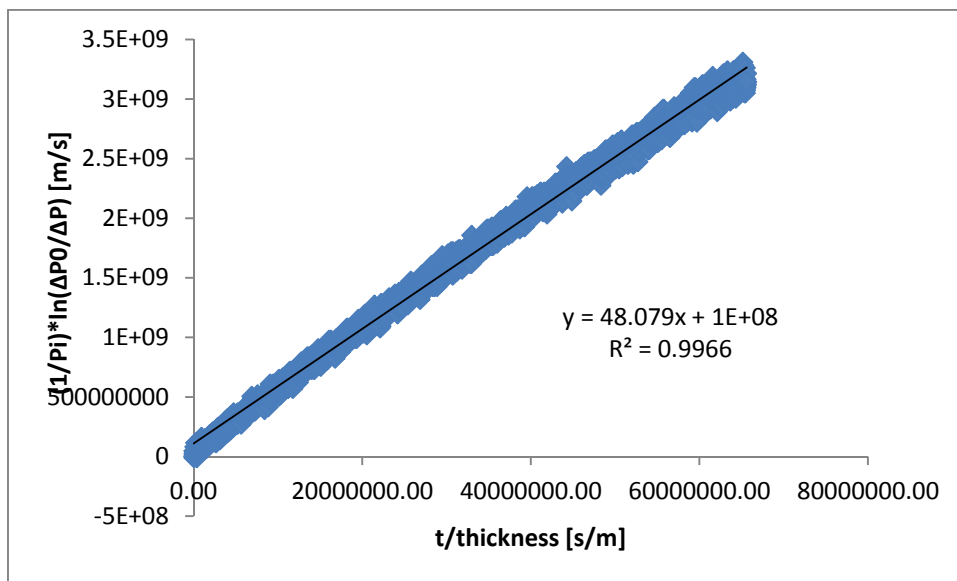


Figure 7. 2. Graphical representation of Eq 3.5.1 where the slope gives the value of  $\beta$

## Appendix II: Estimation of Gas Permeability and Pressure Profiles

The feed and permeate pressure data obtained over time from the software LabView for Matrimid membrane are represented in the Figure 7.3. This graphical representation is for one sample (Matrimid control) with CO<sub>2</sub> and the same procedure was followed for all the membranes and gases tested in this work.

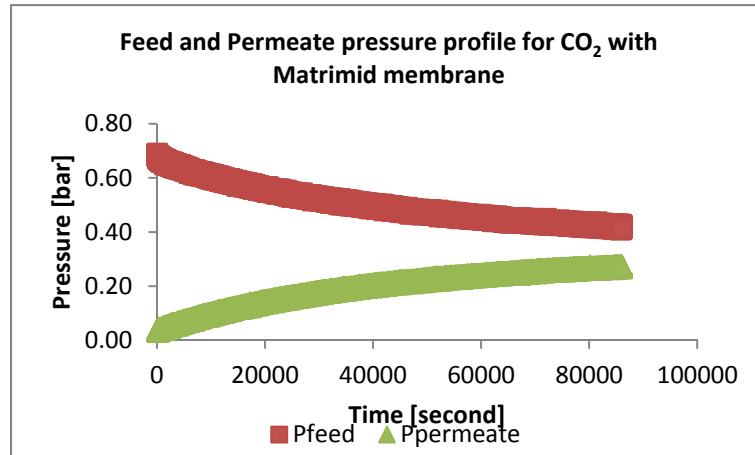


Figure 7. 3. Feed and Permeate pressure profile for CO<sub>2</sub> with Matrimid membrane

By linearizing equation 3.5.1., to the form shown below and using the value  $\beta$  ( $\beta = 48.079$ ) previously calculated (Appendix I) the curve of  $\ln \frac{1}{\beta} \ln \left( \frac{\Delta p_0}{\Delta p} \right)$  versus  $\frac{t}{\delta}$  were traced, the slope of which gives the value of permeability ( $P_{CO_2}$  in [m/s]) as shown in Figure 7.4.

$$\ln \frac{1}{\beta} \ln \left( \frac{\Delta p_0}{\Delta p} \right) = P_{CO_2} \frac{t}{\delta} \dots \dots (Eq 3.5.1)$$

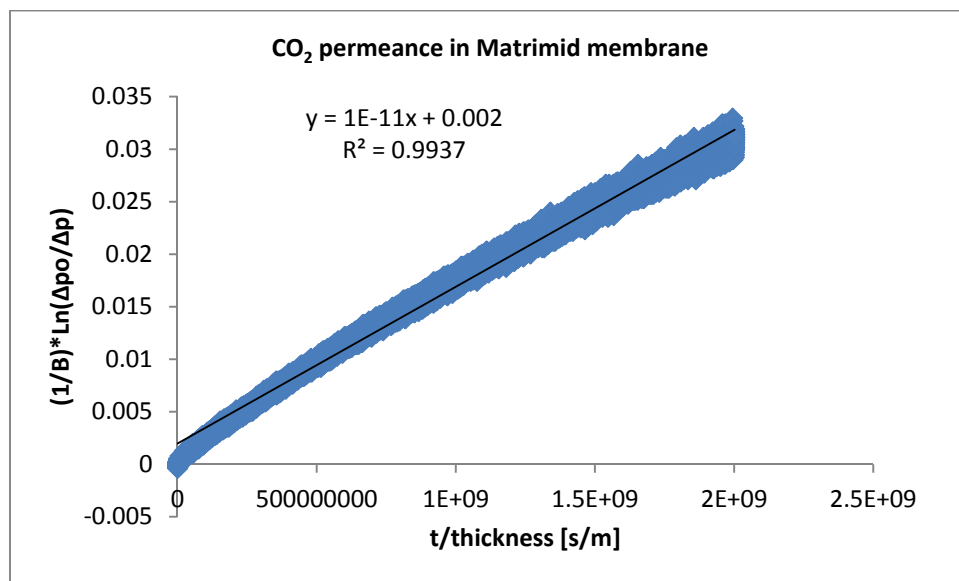


Figure 7. 4. CO<sub>2</sub> permeance in Matrimid membrane

### Appendix III: Puncture test – Stress vs. Strain Curves

Data of *force* and *distance travelled by the probe* is obtained from the software of the TA-xT texture analyser. But no direct interpretations can be made from this data hence it needs to be converted to represent *stress* vs. *strain*. This is done by dividing the *force* data by the probe surface area which gives us the *tension* or *stress* provided by the probe on the sample. The *strain* is calculated from the *distance travelled by probe* as the *elongation of the sample* using the Pythagorean Theorem. A few stress strain curves are shown below. As mentioned earlier, the data of *stress* and *elongation at break* are determined from these curves. The puncture resistance of any material is heavily dependent on the thickness of the sample. Hence care should be taken while comparing the data.

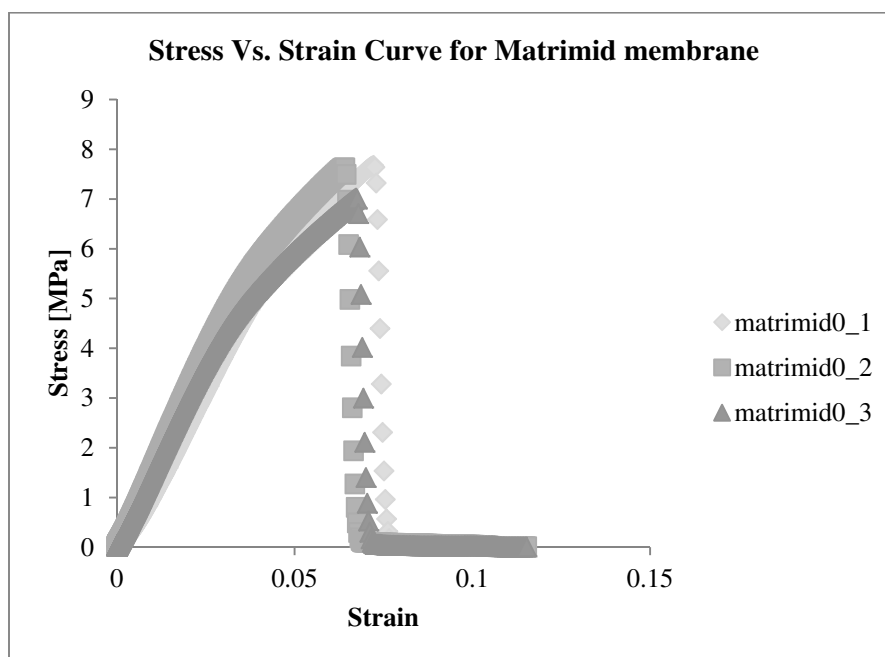


Figure 7. 5. Stress Vs. Strain Curve for Matrimid membrane

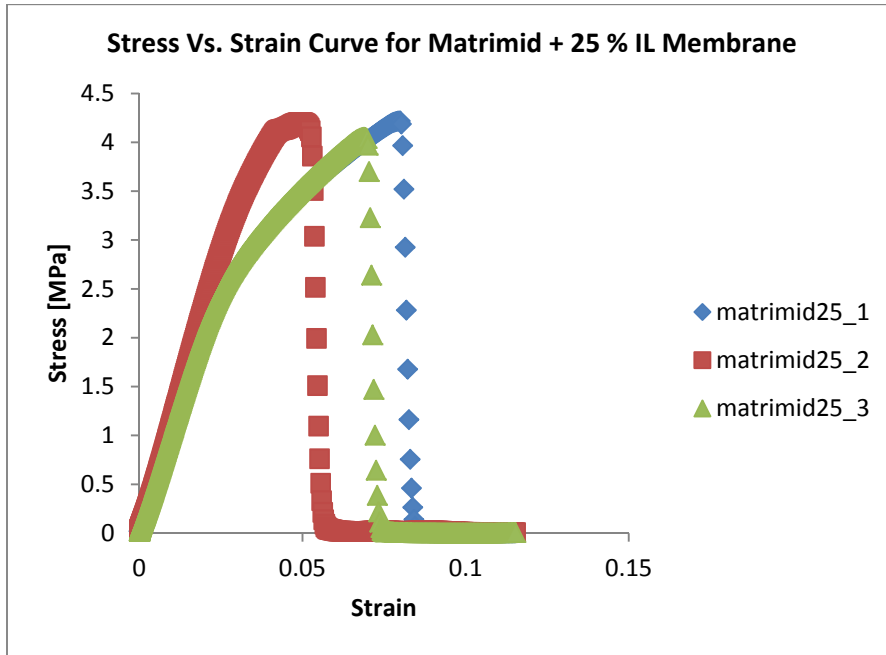


Figure 7. 6. Stress Vs. Strain Curve for Matrimid +25% IL membrane

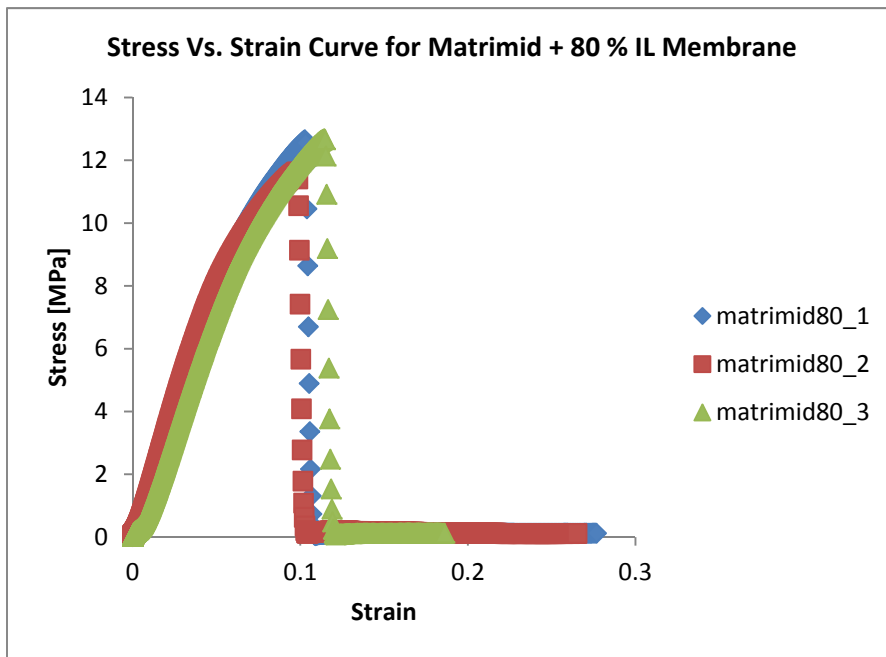


Figure 7. 7. Stress Vs. Strain Curve for Matrimid 80% IL membrane

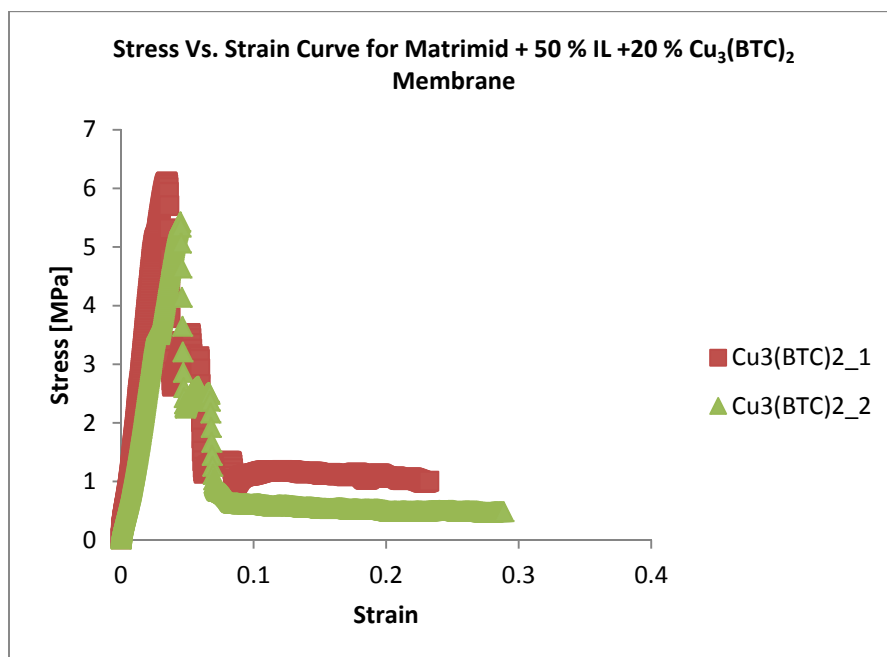


Figure 7. 8. Stress Vs. Strain Curve for Matrimid + 50% IL + 20% Cu<sub>3</sub>(BTC)<sub>2</sub> membrane